Turkish Journal of Earth Sciences (Turkish J. Earth Sci.), Vol. 20, 2011, pp. 655–681. Copyright ©TÜBİTAK
doi:10.3906/yer-0910-43 First published online 03 January 2011

# Growth-invariant Meristic Characters Tools to Reveal Phylogenetic Relationships in Nummulitidae (Foraminifera)

JOHANN HOHENEGGER

University of Vienna, Department of Palaeontology, Althanstraße 14, A-1090 Wien, Austria
(E-mail: johann.hohenegger@univie.ac.at)

*Received 03 November 2009; revised typescript received 04 June 2010; accepted 03 January 2011*

**Abstract:** Morphological characters that are restricted to a few growth-independent characters (such as the embryonic apparatus of nummulitids) or measurements at arbitrarily chosen growth stages (such as the second whorl in planispiral tests) do not adequately explain the phylogenetic relationships of fossil forms. Molecular-genetic investigations enlighten phylogenetic relations, but have two main disadvantages. First, they are restricted to living forms, and second, these relations are based on an extremely small part of the DNA and never on developmental and structural genes that regulate morphology.

Morphometric methods based on growth-invariant characters allow modelling the test shape for each growth stage and thus point to the underlying complex of regulatory and structural genes responsible for shape and size. They can therefore be used in fossil forms.

Growth-independent and growth-invariant parameters were developed to model planispirally enrolled tests using living nummulitids from the West Pacific, where the molecular genetic relations are known. Discriminant analyses based on growth-invariant parameters demonstrate a perfect correlation with biological species. The taxonomic distances (Mahalanobis Distance) indicate phylogenetic relationships and agree well with molecular-genetic relations. The exception is the strong misclassification of the only living representative (*Palaeonummulites*) of the important fossil *Nummulites*-group by molecular genetic methods: that approach places this species with the morphologically completely distinct *Planostegina*-group. The close morphological relation between *O. discoidalis* and *O. ammonoides* and between *O. elegans* and *O. complanata*, both supported by molecular genetic investigation, is an argument for being ecophenotypes of the two biological species *O. ammonoides* and *O. complanata*.

The use of growth-invariant variables and characters can thus be today's strongest tool to shed light on phylogenetic relationships in fossil forms.

**Key Words:** morphometrics, growth-invariant characters, living nummulitids, discriminant analyses

## Foraminifer'lerde Gelişim Boyunca Değişmeyen Karakterlerin Nummulitidae'lerde Filojenetik İlişkilerin Anlaşılması İçin Çalışılması

**Özet:** Gelişim-bağımsız karakterler (örneğin nummulitlerdeki embriyonik aparatüs) ile sınırlanmış birkaç morfolojik özellik veya gelişimin değişik aşamalarında yapılan ölçümler (örneğin planispiral kavkılarda ikinci tur için yapılan ölçümler) fosil foraminifer formlarda filojenetik ilişkilerin açıklanmasında yetersiz kalmaktadır. Bununla beraber, moleküler-genetik çalışmalar bu ilişkileri açıklamakla beraber, iki dezavantajı içermektedir. Öncelikle, bu çalışmalar güncel formlarda uygulanabilmekte olup, açıklanabilen ilişkiler morfolojik gelişimi yönlendiren yapısal genlerden ziyade DNA'nın sadece küçük bir bölümü ile ilgilidir. Gelişim boyunca değişmeyen karakterlerin çalışılmasını içeren morfometrik yöntemler kavkı şeklinin farklı aşamalarda modellenmesine imkan vermekle beraber, foraminifer şekil ve hacmini kontrol eden yapısal genlere işaret ederler ve bu kapsamda sadece fosil formlarda uygulanabilirler.

Bu çalışmada, Batı Pasifik'te moleküler genetik ilişkilerin iyi bilindiği güncel nummulitid'lerde planispiral sarılımlı kavkıların modellenmesi için gelişim-bağımsız parametreler ortaya konmuştur. Bu parametrelere bağlı diskriminant analizleri biyolojik türler ile mükemmel bir korelasyon göstermektedir. Taksonomik mesafeler (Magalanobis mesafesi) filojenetik ilişkileri göstermekte olup moleküler genetik ilişkilerle uyum içerisindedir. Bu duruma tek bir çelişkiyi güncel *Palaeonummulites* oluşturmaktadır: moleküler genetik yöntem ile *Palaeonummulites* morfolojik olarak tamamen farklı olan *Planostegina*-grubu ile eşleşmektedir. Moleküler genetik çalışmalar ile de desteklenen *O. discoidalis* ile *O. ammonoides*, ve *O. elegans* ile *O. complanata* arasındaki yakın morfolojik ilişki *O. ammonoides* ve *O. complanata*'nın

iki biyolojik türün ekofenotipleri olması konusunda temel oluşturmaktadır. Gelişim boyunca sabit kalan değişkenlerin temel alınması fosil formlarda filojenetik ilişkilerin anlaşılmasında en önemli yaklaşımı oluşturmaktadır.

**Anahtar Sözcükler:** morfometri, gelişim boyunca değişmeyen karakterler, güncel nummulitidler, diskriminant analizleri

## Introduction

One of the basic problems in phylogenetic research is the comparability of morphological and molecular-genetic data (e.g., Hayward *et al.* 2004) and the applicability of the latter approach to fossil forms. This leads to comparisons and evaluations of information about phylogenies based on two disparate methods. Most molecular-genetic methods have the advantage that the character set is stable, allowing comparisons and phylogenetic interpretations between taxa of different systematic units such as foraminifera and sponges (Hohenegger 1990). The main disadvantage is the restriction to an extremely small proportion of the cell DNA, mostly ribosomal or mitochondrial DNA, with the further disadvantage of a high probability of homoplasy (convergence – parallelism – reversal) in all nucleotides. Molecular-genetic analyses further neglect information about phylogenetic relationships incorporated in the abundant structural and regulation genes, which are primarily responsible for the formation of morphological characters.

Morphological characters have the disadvantage of instability between organism groups. Together with the differing quality of characters and states (i.e. qualitative characters = attributes, semi-quantitative characters = ranked variables and quantitative = meristic characters), the inter-correlation between characters leads to the problem of character weighting in biological systematics and phylogenetic research (Mayr & Ashlock 1991).

A further problem of morphological characters is their instability during ontogeny, i.e. their dependence on age. This complicates comparisons between individuals of different growth stages, especially in organisms with metamorphosis. Thus, the use of growth-independent and growth-invariant characters, which represent the underlying morphogenetic program of the ontogenetic change and describe the geometry of form more or less completely, is preferable (Hohenegger & Tatzreiter 1992; Hohenegger 1994). Such characters encompass the large complex of regulation and structure genes that are responsible for the development of morphological characters. This approach also allows a better comparison between molecular and morphological data.

The sexual generation (gamonts) of living symbiont-bearing benthic foraminifera of the Nummulitidae are used here to prove the above statements because this family is distinguished by extreme abundance throughout the Cenozoic, combined with radiation and high evolutionary rates, especially during the Paleogene (e.g., Schaub 1981). The Nummulitidae comprise many index fossils used to determine the geological age of tropical shallow water sediments (Serra-Kiel *et al.* 1998). Their continuous occurrence during the Cenozoic makes them excellent objects to demonstrate the phylogeny based on morphogenetic investigations that reflect genetic relationships. Fossil forms can only be studied with morphometric methods because molecular-genetic investigations in foraminifera are restricted to living specimens.

To draw inferences from morphology to the genetic base, the tests of nummulitid foraminifers must not be restricted to a few characters, but should be described in a comprehensive form. This allows geometrical modelling of the complete test. Morphometric investigations based on growth-invariant characters can do this, but detailed information on qualitative characters such as canal systems, pore densities, papillae, plugs, stolons etc. should be incorporated in this method. Such characters are often important for the differentiation between species (e.g., knots in *Operculina ammonoides* versus smooth surface in *O. elegans*) or genera (trabeculae in *Nummulites*). When they are incorporated in phylogenetic analysis, they must be treated as growth-invariant characters (e.g., change of knot size and knot number during growth, additionally regarding the position along the growing test). For the determination of growth-invariant classificatory characters compare the appendix in Hohenegger & Tatzreiter (1992).

Many meristic characters have been measured and used to shed light on phylogenetic trends in nummulitid genera. These range from simple measurements to complex indices relating two or more single measurements to each other. Planispiral nummulitids without chamber partition were characterized by a set of measurements that does not provide complete test reconstruction, but characterizes only a few test properties (Drooger *et al.* 1971; Fermont 1977a). Among these measurements, the largest diameter and total chamber number are growth-dependent, while all measurements from the embryonic apparatus are growth-independent. The outer diameter of the first two whorls characterizing the grade of spiral enrollment is a single growth step and thus not growth-invariant. The number of chambers counted up to the end of the second whorl also represents a growth state and is growth-independent rather than growth-invariant.

Some characters were added characterizing species with chamber partitions (e.g., *Cycloclypeus*, *Heterostegina*), such as the number of chambers without secondary septa including the proloculus and the deuteroloculus, and the number of septula in the 5$^{th}$, 10$^{th}$ and 15$^{th}$ chamber (Fermont 1977b). All these are growth-independent, but not growth-invariant (characterizing change with age). They only allow comparison of specimens at identical, arbitrarily chosen growth stages!

Based on Drooger & Roelofsen (1982), Less *et al.* (2008) and Özcan *et al.* (2009) used similar parameters to describe nummulitids with chamber partitions. They added the index of spiral opening, which relates the difference of two diameters to the difference between the larger diameter and the proloculus. This parameter is the only growth-invariant character that can describe the outer margin at every growth stage, but is restricted to the exponential growth model of the marginal radius.

In his thorough study on *Operculina ammonoides*, Pecheux (1995) used several measurements on the tests, including radius, equatorial surface, chamber number, total volume and chamber volume. He then related these measurements to the whorl number as a time-equivalent parameter. This enabled him to explain the different morphotypes of this species as depending on the depth gradient and substrate.

**Growth-invariant and Growth-independent Characters**

While growth-independent characters are either restricted to the embryonic apparatus or are arbitrarily chosen at defined growth states, growth-invariant characters explain the complete change of the morphological character during ontogeny.

These characters can be described as functions $f$ depending on time $t$. Their constants (parameters) can now be used as growth-invariant parameters. Since most growth functions comprise more than one constant, a single morphological character is almost described by a set of growth-invariant parameters. For example, the linear function

$$f(t) = a + b\,t$$

is characterized by 2 constants: the additive constant $a$ and the multiplicative constant $b$.

But time cannot directly be used as an independent variable in morphometric research (except when studying the morphological change during growth in living individuals). Thus, characters that are monotonously related with time can be used as independent variables. In planispirally enrolled tests of foraminifera, this can either be the chamber number $i$ or the rotation angle $\theta$, where the latter is often characterized as the whorl number. This changes this independent variable from a continuous to a discrete meristic variable.

The following section describes growth-independent and growth-invariant characters (Figure 1) and shows growth functions in representatives of the investigated nummulitid species (Figure 2).

*Proloculus Size* (Figure 1A)

This character, often regarded as very important for detecting phylogenetic lineages in larger foraminifera, is growth-independent per definition. The geometrical mean of proloculus length, width and height should be used as the shape-independent constant characterizing proloculus size of a single specimen

$$ps = (length \times width \times height)^{1/3} \qquad (1)$$

This character can be used in equatorial sections calculating the square root of the product between length and height.

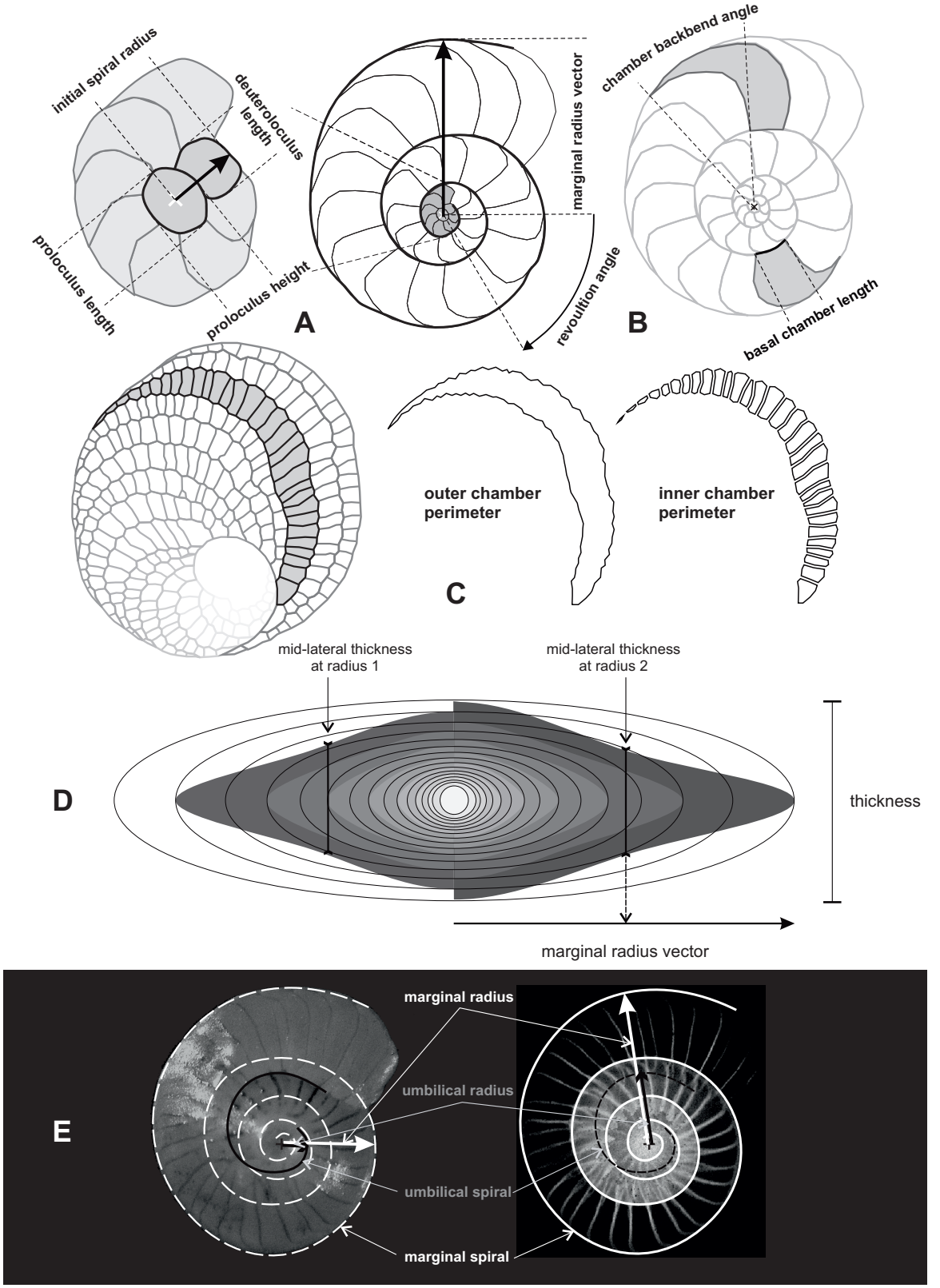


**Figure 1.** Basic measurements of growth-invariant and growth-independent characters (explanation in the text).

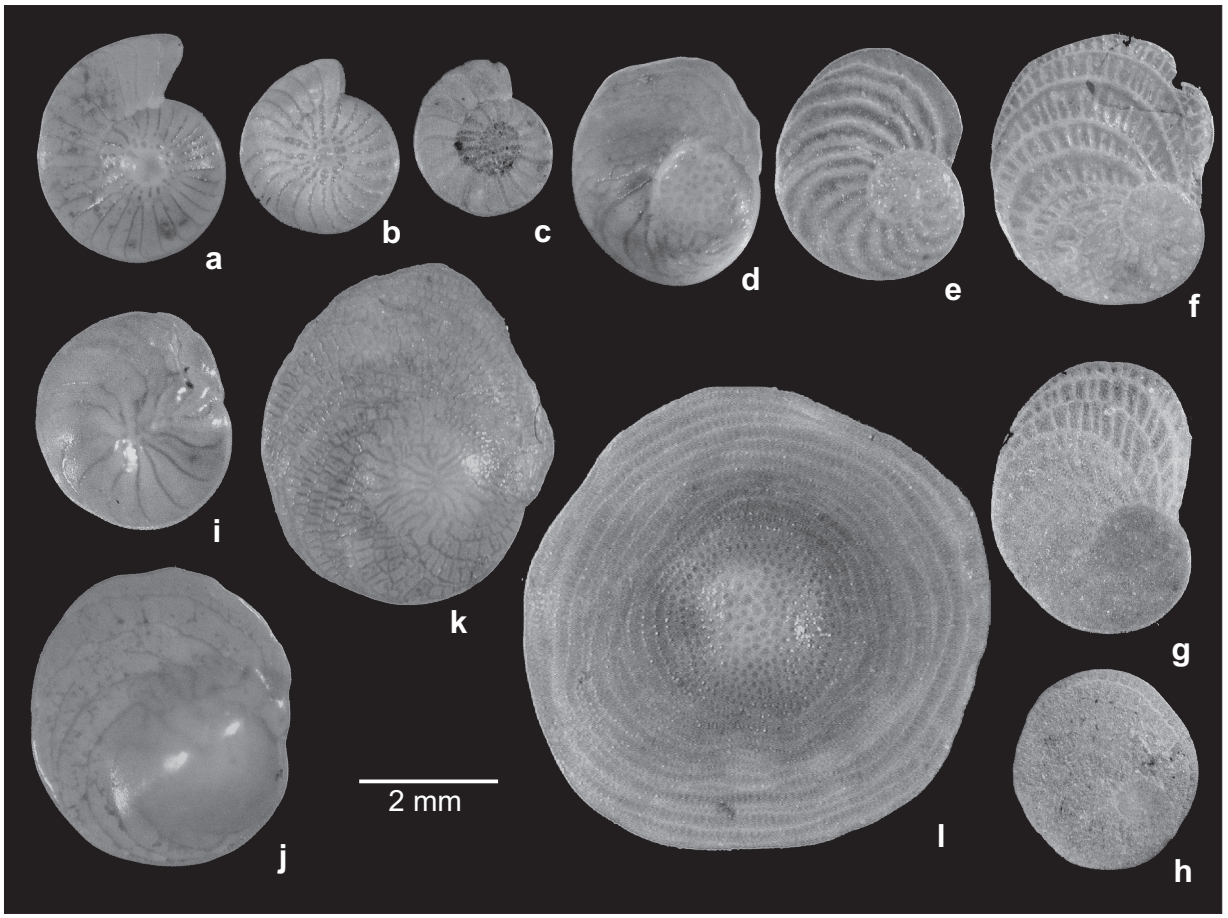


**Figure 2.** Representatives of living nummulitids: **(a)** *Operculina discoidalis* (d'Orbigny), **(b)** *Operculina ammonoides* (Gronovius), **(c)** *Operculina* cf. *ammonoides* (Gronovius), **(d)** *Operculina elegans* (Cushman), **(e)** *Operculina complanata* (Defrance), **(f)** *Planoperculina heterosteginoides* (Hofker), **(g)** *Planostegina longisepta* (Zheng), **(h)** *Planostegina operculinoides* (Hofker), **(i)** *Palaeonummulites venosus* (Fichtel & Moll), **(j)** *Operculinella cumingii* (Carpenter), **(k)** *Heterostegina depressa* d'Orbigny, **(l)** *Cycloclypeus carpenteri* Brady.

*Deuteroloculus Ratio* (Figure 1A)

This parameter, again growth-independent, relates the length of the second chamber to proloculus length, characterizing the deuteroloculus size for a single specimen

$$dr = \frac{length_{deuteroloculus}}{length_{proloculus}} \quad (2)$$

The restriction to a single dimension is justified using deuteroloculus height as the initial parameter of the marginal spiral growth, while deuteroloculus width is incorporated in the later explained growth functions for test thickness.

This parameter can be obtained from equatorial sections.

*Marginal Radius Vector Length* (Figures 1A & 3)

The outline of a planispirally coiled test can be fitted by a rotating vector, where the origin is located in the centre of the proloculus. Because the revolution angle $\theta$ substitutes age, the constants of the function

$$r = b_0(b_1 + b_2\theta)^\theta \quad (3)$$

are growth-invariant. They determine the length of the initial spiral ($b_0$), the expansion rate ($b_1$) and acceleration rate ($b_2$).

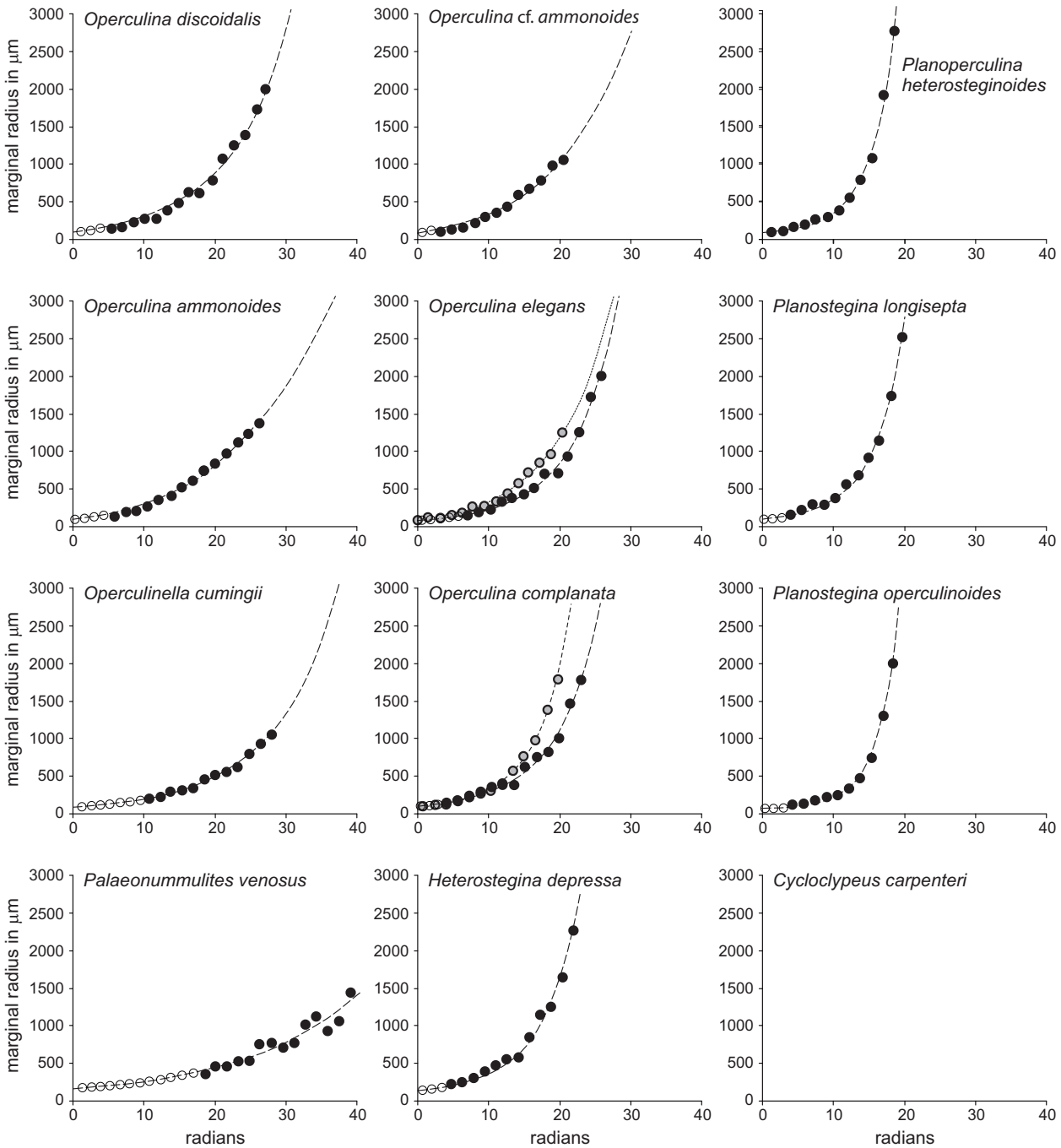


**Figure 3.** Marginal radius vector length dependent on rotation angle. Empirical values of selected specimens fitted by equation (3). Black dots = specimen from 30 m, grey dots = specimen from 70 m.

Excepting cyclic tests of *Cycloclypeus*, the outline of all nummulitids can be perfectly fitted by this function. Again, this parameter is available from equatorial as well as from axial sections.

*Chamber Base Length* (Figures 1B & 4)

This character (Figure 1B) changes with growth, where age is represented by chamber number *i* starting with the second chamber, the deuteroloculus

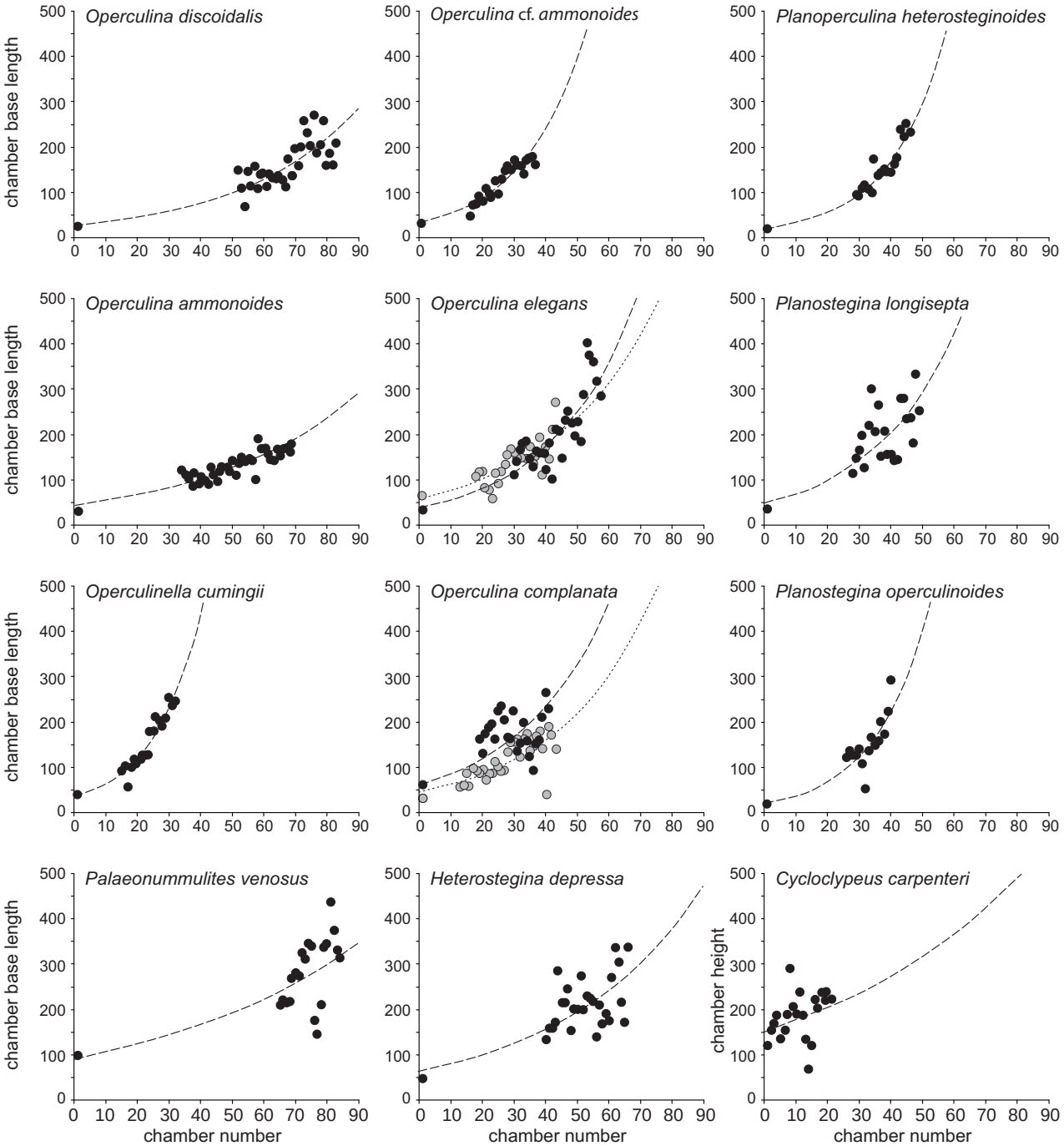


**Figure 4.** Chamber base length dependent on chamber number. Empirical values of selected specimens fitted by equation (4). Black dots = specimen from 30 m, grey dots = specimen from 70 m.

($i$= 1). Empirical data can be fitted by the exponential function

$$h = b_0 \exp(b_1 i) \quad (4)$$

with the two constants $b_0$ indicating the length of the deuteroloculus (Figure 1A) and $b_1$ indicating the expansion rate of the function.

Comparing cyclic tests (*Cycloclypeus*, *Heterocyclina*) with planspirally coiled tests, the chamber height of the cyclic foraminifer, which is homologous with the chamber base length, can be used.

Only equatorial sections allow the determination of this growth function. The fit of empirical data by an exponential function is not as good – but still highly significant – as by the outline. This is due to the strong oscillations in chamber size that could depend on seasonal changes (Figure 4).

*Chamber Backward Bend Angle* (Figures 1B & 5)

This is the angle between the border of the chamber base to the former chamber and the border to the former chamber at the test margin (Figure 1B). Since this angle is restricted to 2π characterizing cyclic chambers in *Cycloclypeus*, the empirical data depending on chamber number $i$ can be fitted by function

$$bba = \frac{1}{1/2\pi + b_0 \exp(b_1 i)} \quad (5)$$

characterized by the constants $b_0$ and $b_1$.

Again, measurements are possible only in equatorial sections.

*Chamber Perimeter Ratio* (Figures 1C & 6)

This character marks the relation between the inner perimeter of a chamber and its outer perimeter (Figure 1C). It indicates the grade of chamber partitions:

$$cpr = \frac{inner\ perimeter}{outer\ perimeter} \quad (6)$$

Character values change during growth, which can be modelled by a function with restricted growth, where the chamber number $i$ represents age

$$cpr_i = \frac{b_0}{1 + b_1 \exp(-b_2 i)} \quad (7)$$

The constant $b_0$ marks the upper limit, $b_1$ the proportion between both perimeters at the deuteroloculus, while $b_2$ represents the growth rate.

Values of $b_0$ mark the grade of chamber partitions (Figure 6). While $b_0 < 1$ is typical for non-partitioned chambers, it approximates 1 in tests with septal undulations (e.g., *Operculina complanata*, *Operculinella cumingii*), becoming > 1 in weakly (e.g., *Planoperculina*) to completely partitioned chambers (e.g., *Cycloclypeus*, *Heterocyclina*, *Heterostegina*, *Planostegina*).

Growth functions can only be obtained from equatorial sections.

*Mid-lateral Thickness* (Figures 1D, 7 & 8)

Test thickness is measured at the axis of rotation. To obtain an approximation of the shape in axial sections, the thickness at the centre of the radius combining the test center with the margin, called here the mid-lateral thickness, is related to the mid-lateral thickness of an ellipse (Figure 1E).

Thickness change with growth can be shown relating the mid-lateral thickness to the marginal radius $r$ representing age. This can be fitted by the function

$$mlth = 0.866\ b_0 \exp\left[\ln r\ (b_1 + b_2 r)\right] \quad (8)$$

where $b_0$ represents the thickness constant, $b_1$ the allometric constant and $b_2$ the restriction rate. The latter constant is a good measure for test flattening because:

- **(i)** $b_2 \sim 0$ determines a section leading to thick or flat lenticular tests (depending on $b_1$) with an elliptical axial section (*Palaeonummulites venosus* in Figure 8)
- **(ii)** $b_2 < 0$ determines test flattening starting with a thick central part (*Heterostegina depressa* in Figure 8)
- **(iii)** $b_2 > 0$ determines test thickening starting with a thinner central part (*Operculina ammonoides* in Figure 8)

This character can be obtained from axial sections.

*Embracing* (Figures 1E & 9)

In planispirally coiled tests the chambers of the last whorl embrace older whorls in different grades, leading from evolute to involute tests. Nummulitid tests can be completely evolute, involute, or transform

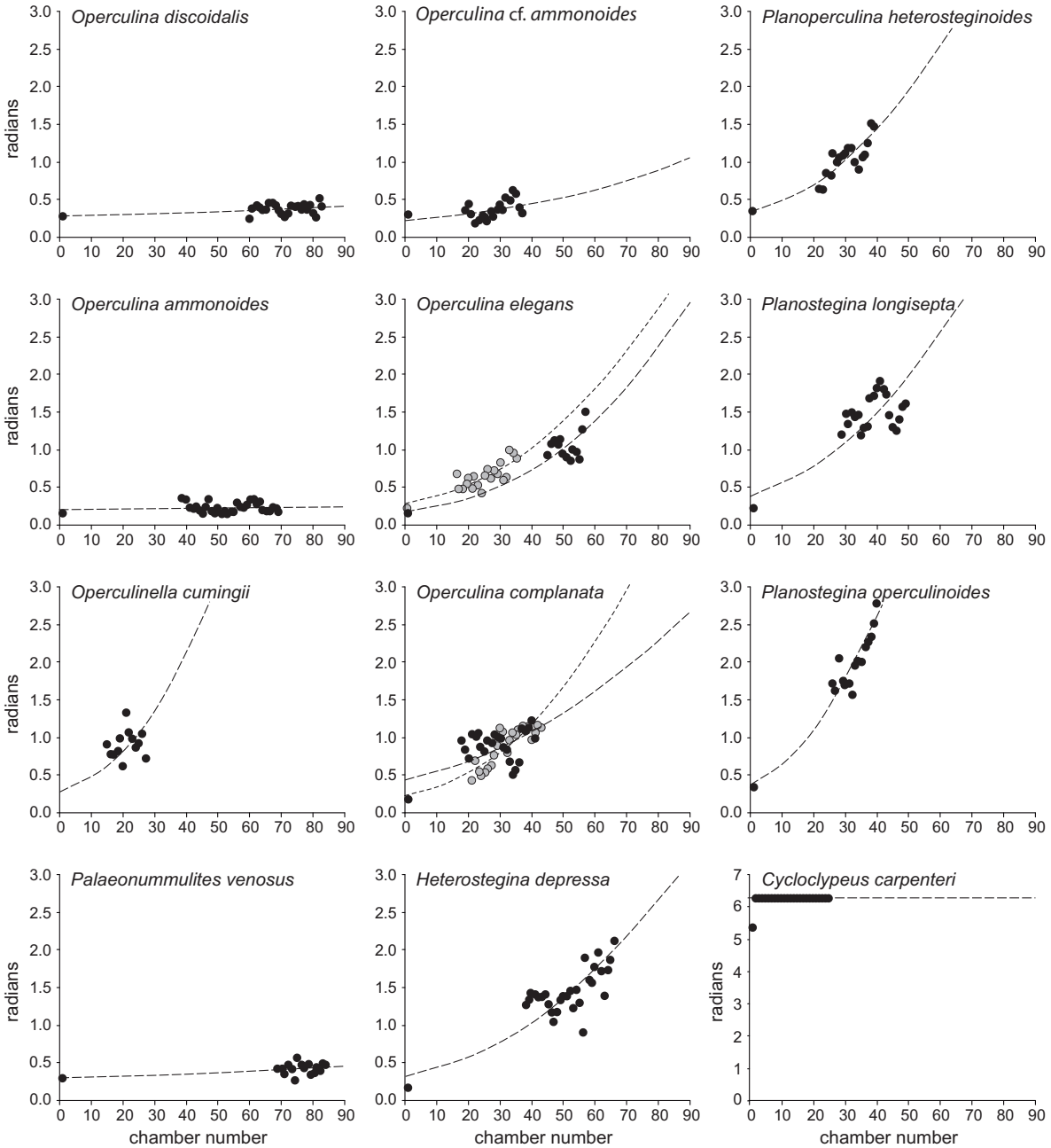


**Figure 5.** Chamber backward bend angle dependent on chamber number. Empirical values of selected specimens fitted by equation (5). Black dots = shallow specimens, grey dots = deep specimens.

from involute to evolute tests (i.e. semi-involute). This can be quantitatively treated by relating the umbilical radius, visible from the outside in semi-involute and evolute tests, to the marginal radius.

The mathematical treatment for determining the grade of embracement during growth is determined by

$$p(\theta) = \left[ f_{marginal}\left(\theta - 2\pi\right) - f_{umbonal}\left(\theta\right) \right] / f_{marginal}\left(\theta - 2\pi\right) \quad (9)$$

The marginal radius in nummulitids can be modelled by equation (3), while the treatment of the umbilical radius is more complex.

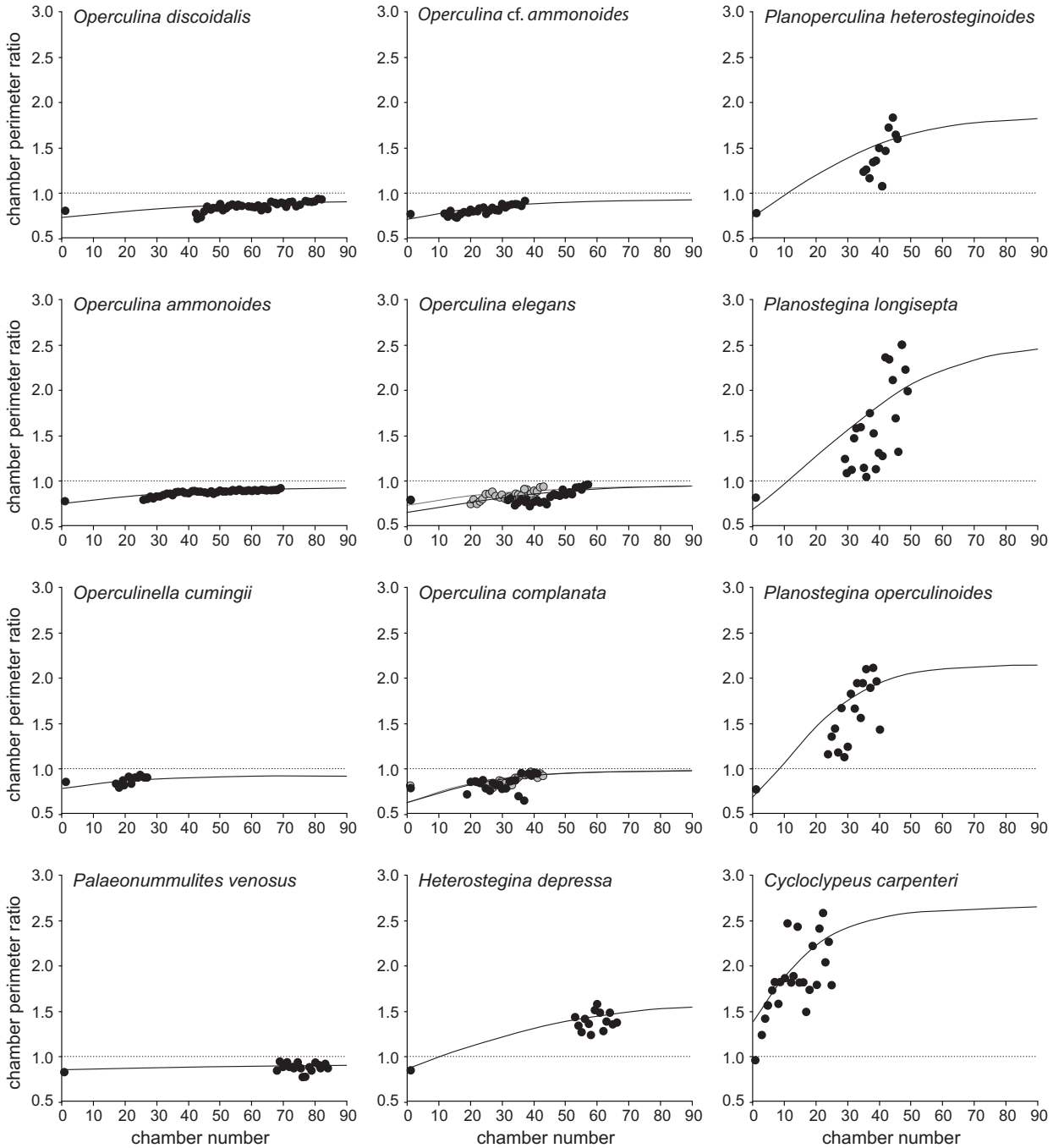


**Figure 6.** Chamber perimeter ratio dependent on chamber number. Empirical values of selected specimens fitted by equation (7). Black dots = shallow specimens, grey dots = deep specimens.

For simplification, a slightly less exact way is proposed. All nummulitids, except cyclic forms, show relationships between both variables during growth that can be modelled by the parabolic function

$$r_{umbonal} = [2p(r_{marginal} - a)]^{1/2} \qquad (10)$$

This relation does not directly show the grade of embracing, because the latter depends on the growth rate of the marginal radius.

Semi-involute and involute tests are characterized by large values of *a*, that characterize the onset

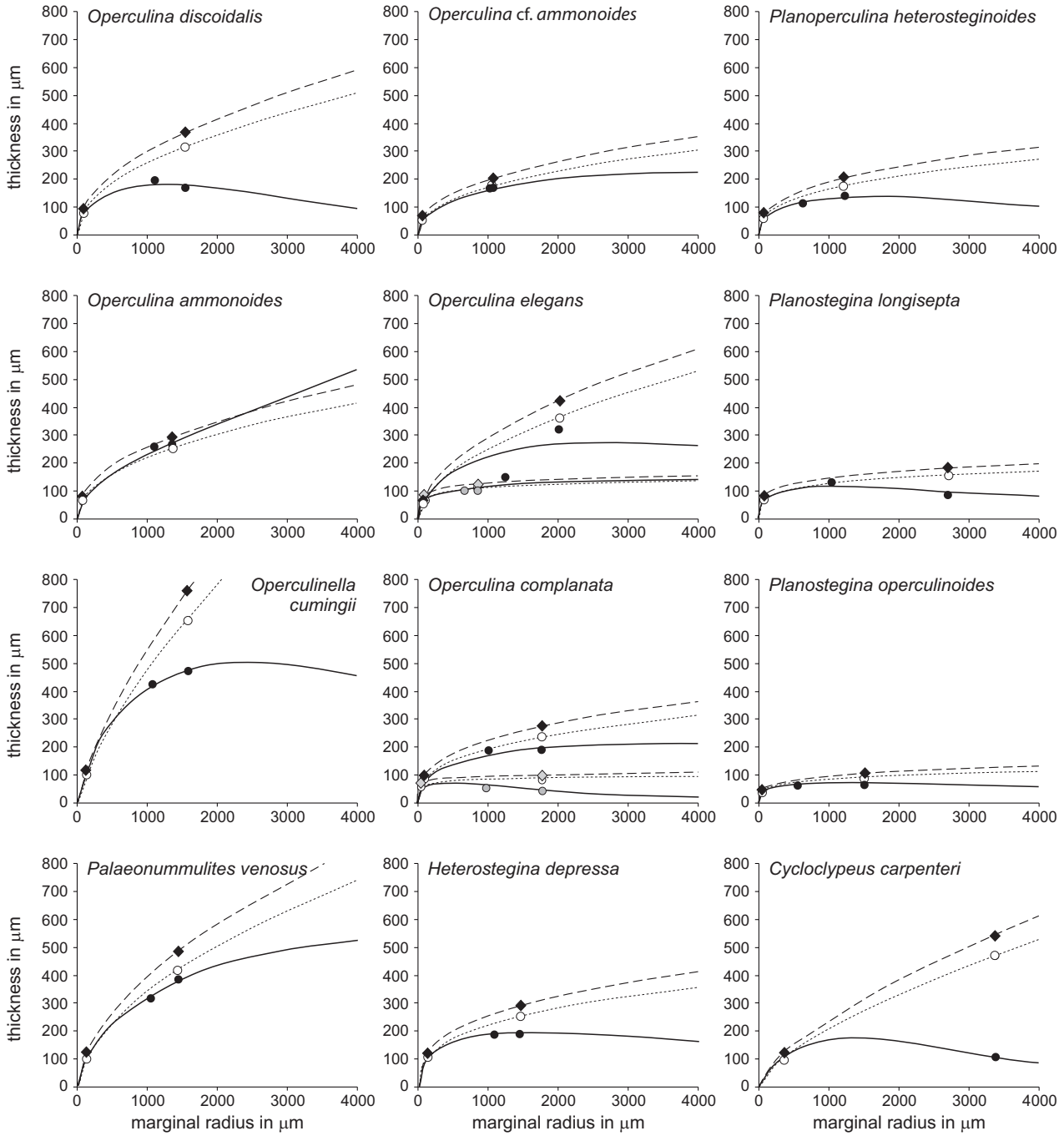


**Figure 7.** Mid-lateral thickness dependent on marginal radius. Empirical values of selected specimens fitted by equation (8). Black dots = shallow specimens, grey dots = deep specimens, white dots= mid-lateral thickness of an ellipse, black rhombs= thickness at the test centre.

of the umbonal radius at a specific length of the marginal radius, while this constant becomes small (approximating 0) in evolute tests. Completely involute tests are determined by

$$a \to \infty.$$

Large values of constant p indicate small differences between the marginal and umbonal radius, while small values reflect large differences

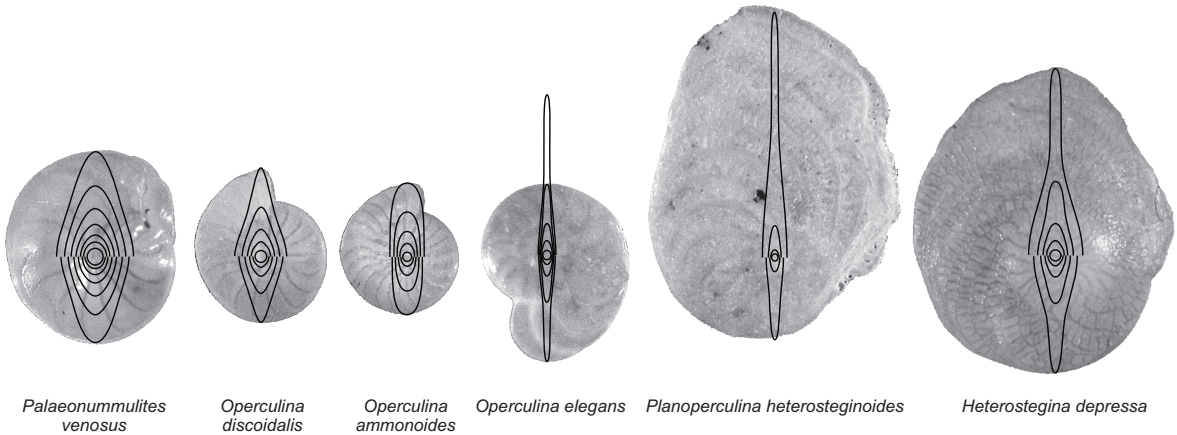


**Figure 8.** Modelling of thickness growth for selected specimens following equation (8).

between both radii, mainly found in species with high expansion rates of the marginal spiral.

Although constant *a* is present in all evolute and large semi-involute tests, its determination is difficult for young individuals of a species with semi-involute tests when the umbonal radius is developed in late growth states, and for involute tests. In comparisons with other species, this scaling problem can be solved for involute tests by substituting the parameter *a* with high values exceeding by far the maximum radius of the species and related forms.

The absent parameter *b* in all involute tests can be replaced by averaging this parameter over species possessing semi-involute tests with similar expansion rates of the marginal radius.

When including cyclic tests like *Cycloclypeus* and *Heterocyclina* in comparative analyses, only the parameter *a* can be used. In such cases, it measures the radius of the tests where all chamberlets of an annular chamber are visible because they are not covered by the thick lamellae of the older chambers. The thick central test parts with invisible chambers and chamberlets can be related to the involute part in spirally coiled nummulitids.

Embracement can be best documented in axial sections.

## Material and Methods

To prove the above methods, the same specimens as published in Hohenegger *et al.* (2000) were measured, together with 4 tests of *Cycloclypeus carpenteri* and 5 tests of *Heterostegina depressa*. Only tests of gamonts (megalospheres, A-generation) were used for species discrimination. Table 1 shows the number of specimens, locations, and depths. Measurements were performed in two ways, as described in Yordanova & Hohenegger (2004). For measuring the grade of evolute coiling and identifying test surface structures, one photograph was taken of each specimen in horizontal projection using the light microscope Nikon Optiphot 2. Chamber form and order were measured on three soft X-ray micrographs (Agfa Structurix D2) taken of each specimen using a Faxitron 43855A. The first micrograph, with short exposure time (5 min at 15 kV), provided information about the outer test part, while the second photograph, with longer exposure time (15 to 20 min at 15 kV), brightened the central test part. A third micrograph (15 to 20 min at 20 kV) was necessary for the innermost part, especially in thick tests. Combining the three micrographs using the graphic program Corel 11 enabled the investigation of internal test structures from the proloculus to the periphery.

All measurements in equatorial section and horizontal projection could be processed using the Kontron 400 Image Analysing System. Measurements of the umbilical and marginal radii (Figure 1A, E) were taken at 1/2 radians, while the other parameters, except for test thickness, were measured for each chamber using the combined X-ray micrographs.

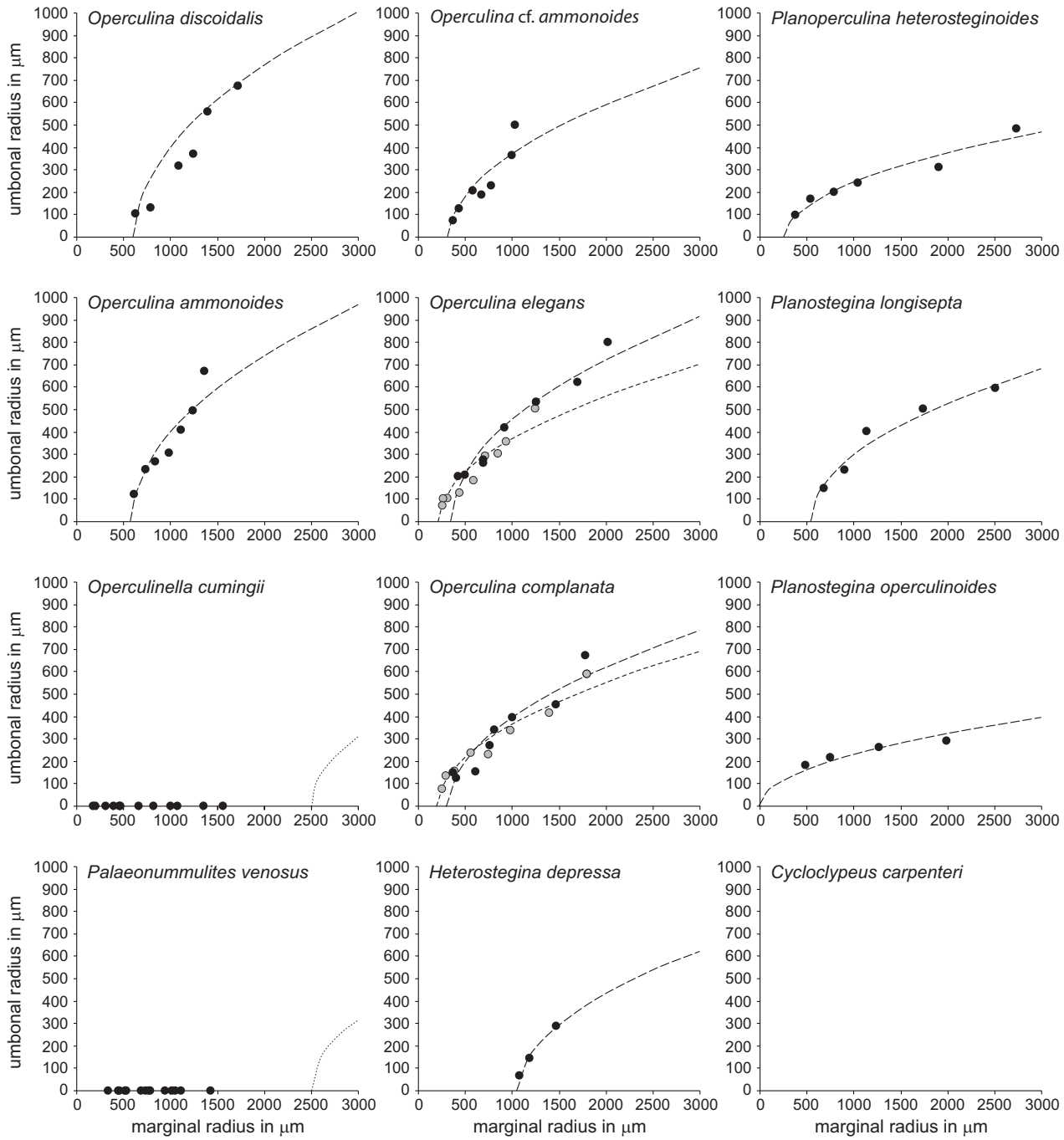


**Figure 9.** Relation between umbonal radius and marginal radius. Empirical values of selected specimens fitted by equation (10). Black dots = shallow specimens, grey dots = deep specimens.

Test thickness was optically measured at the proloculus and at both midpoints of the largest diameter between the test centre and the margin. The electronic spindle Mitutuyo, installed on the light microscope, was used, whereby the measuring points were focused opposed to the base plane.

Basic statistical calculations were performed in Microsoft Excel, while the programs SPSS 15 and

**Table 1.** Location, water depth and number of specimens used for morphogenetic investigation.

| | specimens | location | depth |
|---|---|---|---|
| *Operculinella cumingii* | 5 | Sesoko Jima | 50 m |
| *Nummulites venosus* | 5 | Sesoko Jima | 50 m |
| *Operculina discoidalis* | 3 | Belau | 30 m |
| | 4 | Motobu Peninsula | 18 m |
| *Operculina ammonoides* | 3 | Motobu Peninsula | 18 m |
| *Operculina* c.f. *ammonoides* | 4 | Amakusa Jima | 30 m |
| *Operculina elegans* | 4 | Sesoko Jima | 30 m |
| | 3 | | 70 m |
| *Operculina complanata* | 1 | Sesoko Jima | 30 m |
| | 4 | | 70 m |
| | 8 | | 90 m |
| *Planoperculina heterosteginoides* | 7 | Sesoko Jima | 90 m |
| *Planostegina longisepta* | 4 | Sesoko Jima | 90 m |
| *Planostegina operculinoides* | 4 | Sesoko Jima | 90 m |
| *Heterostegina depressa* | 5 | Sesoko Jima | 50 m |
| *Cycloclypeus carpenteri* | 6 | Ishigaki Jima | 60 m |

PAST (Hammer *et al.* 2001) were used for complex analyses (e.g., nonlinear regression, multivariate analyses).

## Morphological Relationships

Two important questions can be answered using growth-invariant morphometric characters. The first asks for the concordance between species of larger foraminifera based, on the one side, on population structure and population dynamics of living specimens and, on the other, on morphology. When this concordance is high, then the biological species can be detected by morphometric analysis even in fossil forms. The second question applies to the phylogenetic relationships between species based on growth-invariant morphological characters, because the change of characters is caused by environmental and genetic factors. The influence of environmental factors such as gradient dependence (e.g., light intensity), where the organisms respond through changes in (functional) morphological characters, must be separated from environment-independent characters (Hohenegger 2000, 2004).

Both questions can simultaneously be treated using discriminant analysis (Sneath & Sokal 1973; Krzanowski & Marriott 1995), where the resulting Mahalanobis Distances between groups centres hint at the intensities of morphological relationships. These relations may reflect phylogenetic relations, but must not be regarded as direct connections.

Unlike classification analyses (cluster analyses), which create classes homogeneous in their character set, discriminant analysis is based on *a priori* defined classes (Sneath & Sokal 1973). Discriminant

analysis specifies the characters suited best for differentiating between classes. At the same time, a proof of the *a priori* allocation of specimens to the species group according to the character set is given. Other individuals, not incorporated in the primary analyses, can be allocated to the nearest class, but do not necessarily become a member of this group.

Two discriminant analyses were calculated. The first is restricted to species with spiral tests, where all mentioned 17 growth-invariant characters could be used. The second analysis includes the cyclic *Cyclcoclypeus carpenteri*, which has annular tests, thus restricting the character set to 11; this allows the comparison of all living nummulitids (*Heterocyclina* is not included in this investigation).

The discriminant analysis of spiral forms based on 17 growth-invariant characters (Table 2) was perfect, explaining 86% of the total variance by the first 2 discriminant functions; the remaining 10 axes are of negligible importance (Table 3). Furthermore, the allocation of individuals based on morphometric characters to the predicted biological species is also perfect, with no misclassification (Table 4). Thus, the graphical representation of individuals within the 2-dimensional space represented by the first and second discriminant functions allows a good graphical picture of the biological species differentiation.

The structure matrix shows the importance of characters by their correlation with discriminant functions (Table 5). The first function, explaining 64.2% of total variance, is extremely positively correlated with the parameter *a* of equation (9), indicating the onset of evolute coiling. The significant negative correlation of the two important parameters describing chamber partitioning (equation 7), with the first discriminant function separating strong involute forms such as *Palaeonummulites venosus* and *Operculinella cumingii* with no chamber partitions from evolute forms with extreme chamber partitions such as *Planoperculina* and *Planostegina* (Figure 10A).

The second discriminant function strengthens the importance of chamber partitioning by its significant negative correlation with all three parameters describing the grade of chamber partitioning. Here, parameter *a* of equation (9), indicating the onset of evolute coiling and the initial grade of chamber indicating backwards bending ($b_0$ of equation 5) are significantly positively correlated with the second discriminant function. Therefore, beyond separating involute (*Palaeonummulites*, *Operculinella*), semi-involute (*Heterostegina*, *Operculina ammonoides*, *O. discoidalis*) and evolute coiling (*O. elegans*, *O. complanata*, *Planoperculina, Planostegina*) as demonstrated by the first function, the second function confirms that chamber partition is combined with greater chamber backward bending. This explains the transition from *O.* cf. *ammonoides*, *O. ammonoides* and *O. discoidalis* with weak backward bending to species with the strongest backward bend, as represented by *Operculinella*, *Heterostegina*, *Planoperculina* and *Planostegina* (Figure 10A).

Table 5 shows the importance of characters – in decreasing order – for discriminating species groups. As well as the above-mentioned characters, the expansion rate of the marginal radius (parameter $b_1$ of equation 3) is important. The minimum spanning tree of squared Mahalanobis distances based on all discriminant functions shows the morphogenetically shortest connections between species, possibly reflecting phylogenetic relationships (Figure 10B). *Operculina ammonoides* and *O. discoidalis* are closely related, while the differentiation between *O. elegans* and *O. complanata,* based solely on septal undulation, cannot be verified through complex morphogenetic analysis. This is because the shallow-living groups of both species are more closely related to each other than to their deeper-living partners, whereby both deeper-living groups are also closely connected. Nevertheless, all 4 groups are clearly separated from the *O. ammonoides* – *O. discoidalis* group. The intermediate *O.* cf. *ammonoides* from Japan is more connected to the *O. ammonoides* group. *Planoperculina heterosteginoides* and the two *Planostegina* species comprise a separate group that is related to the deeper-living *O. complanata*, while *H. depressa* is loosely connected to the shallow-living *O. elegans* and to *O. discoidalis*. *Palaeonummulites vensosus* and *O. cumingii* are grouped together, whereby the latter species shows a weak relationship to *H. depressa*.

*Cycloclypeus carpenteri* is included in the second discriminant analysis. This reduces the

**Table 2.** Statistical parameters of growth-independent characters and growth-invariant parameters.

| | | pro loculus size | deutero loculus ratio | marginal radius | | | basal chamber length | | chambers backward bend | | mediolateral thickness | | | chambers perimeter ratio | | | embracing | |
|---|---|---|---|---|---|---|---|---|---|---|---|---|---|---|---|---|---|---|
| | | | | $b_0$ | $b_1$ | $b_2$ | $b_0$ | $b_1$ | $b_0$ | $b_1$ | $b_0$ | $b_1$ | $b_2$ | $b_0$ | $b_1$ | $b_2$ | a | p |
| *Palaeonummulites venosus* | Mean | 117.9 | 0.86 | 141.8 | 1.07 | 0.42 | 102.3 | 0.021 | 0.986 | 4.14 | 7.15 | 0.603 | -0.254 | 0.908 | 0.152 | 0.159 | *2000* | *100* |
| | SD | *15.7* | *0.18* | *13.6* | *0.01* | *3.31* | *54.8* | *0.011* | *0.007* | *0.68* | *2.70* | *0.083* | *0.158* | *0.030* | *0.131* | *0.172* | | |
| *Operculinella cumingii* | Mean | 108.6 | 0.88 | 123.8 | 1.07 | 19.31 | 105.1 | 0.045 | 0.943 | 3.92 | 6.36 | 0.626 | -0.340 | 0.955 | 0.192 | 0.487 | *2000* | *100* |
| | SD | *16.0* | *0.18* | *23.8* | *0.04* | *18.87* | *60.8* | *0.019* | *0.035* | *1.15* | *3.38* | *0.096* | *0.206* | *0.047* | *0.051* | *0.063* | | |
| *Operculina discoidalis* | Mean | 96.1 | 0.77 | 106.7 | 1.10 | 1.19 | 45.1 | 0.019 | 0.997 | 4.23 | 9.51 | 0.512 | -0.437 | 0.933 | 0.263 | 0.231 | 778.6 | 272.3 |
| | SD | *16.7* | *0.12* | *15.2* | *0.01* | *5.32* | *12.1* | *0.005* | *0.006* | *0.79* | *2.36* | *0.074* | *0.197* | *0.018* | *0.128* | *0.116* | *173.1* | *113.0* |
| *Operculina ammonoides* | Mean | 85.9 | 0.90 | 93.9 | 1.14 | -11.59 | 41.6 | 0.023 | 0.997 | 4.34 | 11.00 | 0.472 | 0.121 | 0.917 | 0.182 | 0.340 | 668.5 | 194.7 |
| | SD | *4.4* | *0.05* | *3.4* | *0.02* | *6.09* | *5.2* | *0.002* | *0.002* | *0.84* | *3.94* | *0.082* | *0.051* | *0.014* | *0.044* | *0.132* | *107.2* | *73.9* |
| *Operculina ?ammonoides* | Mean | 89.5 | 0.77 | 95.7 | 1.15 | -9.33 | 40.4 | 0.038 | 0.991 | 3.92 | 43.77 | 0.205 | -0.080 | 0.925 | 0.226 | 0.437 | 308.4 | 122.5 |
| | SD | *23.7* | *0.19* | *23.5* | *0.02* | *4.84* | *9.4* | *0.009* | *0.008* | *1.17* | *25.26* | *0.145* | *0.080* | *0.006* | *0.063* | *0.134* | *87.3* | *40.3* |
| *Operculina elegans* (shallow) | Mean | 90.1 | 0.86 | 112.7 | 1.11 | 8.98 | 55.4 | 0.033 | 0.973 | 3.43 | 10.57 | 0.476 | -0.335 | 0.940 | 0.430 | 0.478 | 354.8 | 137.4 |
| | SD | *30.6* | *0.07* | *44.8* | *0.01* | *9.23* | *25.2* | *0.018* | *0.014* | *1.57* | *3.09* | *0.083* | *0.088* | *0.038* | *0.108* | *0.144* | *153.6* | *55.7* |
| *Operculina elegans* (deep) | Mean | 84.1 | 0.79 | 93.6 | 1.13 | 2.12 | 46.4 | 0.035 | 0.973 | 3.24 | 32.92 | 0.214 | -0.355 | 0.976 | 0.509 | 0.520 | 197.1 | 75.2 |
| | SD | *7.5* | *0.15* | *10.8* | *0.02* | *5.92* | *13.3* | *0.005* | *0.010* | *0.95* | *6.81* | *0.046* | *0.519* | *0.063* | *0.234* | *0.124* | *42.2* | *16.2* |
| *Operculina complanata* (shallow) | Mean | 89.4 | 0.88 | 101.6 | 1.09 | 15.09 | 72.4 | 0.025 | 0.975 | 3.19 | 21.01 | 0.417 | -0.345 | 1.016 | 0.541 | 0.379 | 391.9 | 119.5 |
| | SD | *21.1* | *0.15* | *26.5* | *0.02* | *4.55* | *11.9* | *0.006* | *0.006* | *1.32* | *24.40* | *0.204* | *0.188* | *0.073* | *0.144* | *0.124* | *59.1* | *24.3* |
| *Operculina complanata* (deep) | Mean | 76.0 | 1.01 | 86.2 | 1.12 | 26.11 | 38.3 | 0.043 | 0.965 | 2.89 | 37.43 | 0.190 | -0.280 | 0.976 | 0.666 | 0.703 | 257.2 | 85.6 |
| | SD | *15.8* | *0.10* | *16.8* | *0.02* | *15.74* | *11.8* | *0.007* | *0.008* | *0.73* | *21.21* | *0.110* | *0.240* | *0.025* | *0.118* | *0.057* | *63.6* | *19.8* |
| *Planoperculina heterosteginoides* | Mean | 76.8 | 0.85 | 89.5 | 1.10 | 61.68 | 27.0 | 0.060 | 0.945 | 3.61 | 28.35 | 0.253 | -0.187 | 1.786 | 1.348 | 0.731 | 226.0 | 53.3 |
| | SD | *13.3* | *0.17* | *14.3* | *0.05* | *38.10* | *8.4* | *0.009* | *0.017* | *0.58* | *12.66* | *0.102* | *0.145* | *0.200* | *0.249* | *0.202* | *93.5* | *20.2* |
| *Planostegina longisepta* | Mean | 94.3 | 0.76 | 102.6 | 1.11 | 43.06 | 46.9 | 0.040 | 0.949 | 2.92 | 35.07 | 0.222 | -0.339 | 2.228 | 2.025 | 0.565 | 290.9 | 74.7 |
| | SD | *13.7* | *0.05* | *7.5* | *0.01* | *13.74* | *5.5* | *0.004* | *0.009* | *0.70* | *8.96* | *0.032* | *0.260* | *0.306* | *0.556* | *0.063* | *187.4* | *32.7* |
| *Planostegina operculinoides* | Mean | 53.6 | 0.87 | 68.4 | 1.08 | 98.89 | 25.0 | 0.061 | 0.935 | 2.16 | 18.96 | 0.286 | -0.261 | 2.305 | 2.308 | 0.969 | 60.2 | 28.5 |
| | SD | *9.5* | *0.16* | *14.1* | *0.04* | *18.51* | *6.9* | *0.010* | *0.008* | *0.43* | *10.84* | *0.127* | *0.132* | *0.261* | *0.186* | *0.305* | *88.0* | *7.9* |
| *Heterostegina depressa* | Mean | 113.4 | 0.76 | 115.6 | 1.10 | 10.47 | 66.6 | 0.019 | 0.968 | 3.41 | 14.44 | 0.440 | -0.374 | 1.746 | 1.171 | 0.369 | 1135.6 | 98.7 |
| | SD | *27.6* | *0.07* | *24.9* | *0.02* | *10.80* | *15.4* | *0.006* | *0.008* | *0.93* | *4.49* | *0.053* | *0.204* | *0.239* | *0.228* | *0.107* | *297.8* | *9.1* |
| *Cycloclypeus carpenteri* | Mean | 364.6 | 1.64 | | | | 133.9 | 0.022 | | | 37.51 | 0.334 | -0.362 | 2.628 | 0.929 | 0.813 | 1370.2 | |
| | SD | *91.3* | *0.21* | | | | *33.1* | *0.010* | | | *18.91* | *0.068* | *0.119* | *0.071* | *0.151* | *0.408* | *190.8* | |

**Table 3.** Discriminant analysis based on all variables: eigenvalues and variance proportion.

| discriminant function | eigenvalue | % of variance | cumulative % | canonical correlation |
|---|---|---|---|---|
| 1 | 67.311 | 64.2 | 64.2 | 0.993 |
| 2 | 22.878 | 21.8 | 86.0 | 0.979 |
| 3 | 5.931 | 5.7 | 91.7 | 0.925 |
| 4 | 4.168 | 4.0 | 95.6 | 0.898 |
| 5 | 1.843 | 1.8 | 97.4 | 0.805 |
| 6 | 0.971 | 0.9 | 98.3 | 0.702 |
| 7 | 0.741 | 0.7 | 99.0 | 0.652 |
| 8 | 0.499 | 0.5 | 99.5 | 0.577 |
| 9 | 0.313 | 0.3 | 99.8 | 0.488 |
| 10 | 0.110 | 0.1 | 99.9 | 0.315 |
| 11 | 0.080 | 0.1 | 100.0 | 0.272 |
| 12 | 0.026 | 0.0 | 100.0 | 0.159 |

character space to 11 dimensions (Table 6). The first 2 discriminant functions explain 82.6% of total variance. In contrast to the former analysis, however, the 3rd function gains additional importance, with 10.3% variance proportion.

The separation between the biologically defined groups by growth-invariant characters is not as good as in the former analyses because all characters describing spiral growth and the backbending of chambers are excluded. Nevertheless, the allocation of individuals to biologically defined species based on discriminant functions is good, with 5 misclassifications and 66 correct allocations (Table 7).

Quite similar to the first analyses, both main parameters indicating chamber partitioning are significantly negatively correlated with the first function; the onset of evolute coiling retains its strong positive correlation (Table 8). Therefore, the order of individuals along the first axis is quite similar to the former analysis (Figure 11A). The second discriminant function is now positively correlated with both parameters indicating the onset of evolute coiling together with the upper limit of the chamber perimeter ratio (parameter $b_0$ of equation 7). Also positively correlated is proloculus size. This leads to the strong separation of *C. carpenteri* from the other nummulitids, although the cyclic arrangement of chambers (leading to the lack of parameters for backward bend of chambers) and spiral growth are not incorporated.

The minimum spanning tree constructed using squared Mahalanobis distances based on all 11 discriminant functions shows the morphological connections between species. These relations are very similar to those represented in the first discriminant analysis. The main differences are the close connection of *O.* cf. *ammonoides* from Japan to the deep *O. elegans* (both are flat) as well as the weak, but shortest connection from *P. venosus* to *O. discoidalis* and the shortest connection from *H. depressa* to *O. discoidalis*. The most important result in this analysis is the closest, but weak connection of the cyclic *C. carpenteri* to *H. depressa*.

**Differentiation Between Species**

Discriminant analysis showed the morphological relationships between species, yielding 4 distinct clusters:

1. *Palaeonummulites venosus – Operculinella cumingii*
2. *Operculina discoidalis – O. ammonoides – O.* cf. *ammonoides*
3. *Operculina elegans – O. complanata*
4. *Planoperculina heterosteginoides – Planostegina longisepta – P. operculinoides*

with *Heterostegina depressa* as an intermediate form and *Cycloclypeus carpenteri* as an outlier. Differences of species within clusters were tested by analyses of variance (Tables 9–11).

According to this method, *Palaeonummulites venosus* and *Operculinella cumingii* are differentiated by chamber base length; in the latter species, the chambers become higher during growth. A further significant difference is the grade of chamber backbend, which is also higher in *O. cumingii*. Significant differences in the increase rate of the

**Table 4.** Discriminant analysis based on all variables. Comparison of the original (a priori) classification with the predicted classification.

| | | species | predicted classification | | | | | | | | | | | | | total |
|---|---|---|---|---|---|---|---|---|---|---|---|---|---|---|---|---|
| | | | *Palaeonummulites venosus* | *Operculinella cumingii* | *Operculina discoidalis* | *Operculina ammonoides* | *Operculina ?ammonoides* | *Operculina elegans* (shallow) | *Operculina elegans* (deep) | *Operculina complanata* (shallow) | *Operculina complanata* (deep) | *Planoperculina heterosteginoides* | *Planostegina longisepta* | *Planostegina operculinoides* | *Heterostegina depressa* | |
| original classification | number | *Palaeonummulites venosus* | 4 | 0 | 0 | 0 | 0 | 0 | 0 | 0 | 0 | 0 | 0 | 0 | 0 | 4 |
| | | *Operculinella cumingii* | 0 | 5 | 0 | 0 | 0 | 0 | 0 | 0 | 0 | 0 | 0 | 0 | 0 | 5 |
| | | *Operculina discoidalis* | 0 | 0 | 10 | 0 | 0 | 0 | 0 | 0 | 0 | 0 | 0 | 0 | 0 | 10 |
| | | *Operculina ammonoides* | 0 | 0 | 0 | 3 | 0 | 0 | 0 | 0 | 0 | 0 | 0 | 0 | 0 | 3 |
| | | *Operculina ?ammonoides* | 0 | 0 | 0 | 0 | 4 | 0 | 0 | 0 | 0 | 0 | 0 | 0 | 0 | 4 |
| | | *Operculina elegans* (shallow) | 0 | 0 | 0 | 0 | 0 | 5 | 0 | 0 | 0 | 0 | 0 | 0 | 0 | 5 |
| | | *Operculina elegans* (deep) | 0 | 0 | 0 | 0 | 0 | 0 | 3 | 0 | 0 | 0 | 0 | 0 | 0 | 3 |
| | | *Operculina complanata* (shallow) | 0 | 0 | 0 | 0 | 0 | 0 | 0 | 5 | 0 | 0 | 0 | 0 | 0 | 5 |
| | | *Operculina complanata* (deep) | 0 | 0 | 0 | 0 | 0 | 0 | 0 | 0 | 8 | 0 | 0 | 0 | 0 | 8 |
| | | *Planoperculina heterosteginoides* | 0 | 0 | 0 | 0 | 0 | 0 | 0 | 0 | 0 | 7 | 0 | 0 | 0 | 7 |
| | | *Planostegina longisepta* | 0 | 0 | 0 | 0 | 0 | 0 | 0 | 0 | 0 | 0 | 4 | 0 | 0 | 4 |
| | | *Planostegina operculinoides* | 0 | 0 | 0 | 0 | 0 | 0 | 0 | 0 | 0 | 0 | 0 | 4 | 0 | 4 |
| | | *Heterostegina depressa* | 0 | 0 | 0 | 0 | 0 | 0 | 0 | 0 | 0 | 0 | 0 | 0 | 5 | 5 |
| | percentages | *Palaeonummulites venosus* | 100 | 0 | 0 | 0 | 0 | 0 | 0 | 0 | 0 | 0 | 0 | 0 | 0 | 100 |
| | | *Operculinella cumingii* | 0 | 100 | 0 | 0 | 0 | 0 | 0 | 0 | 0 | 0 | 0 | 0 | 0 | 100 |
| | | *Operculina discoidalis* | 0 | 0 | 100 | 0 | 0 | 0 | 0 | 0 | 0 | 0 | 0 | 0 | 0 | 100 |
| | | *Operculina ammonoides* | 0 | 0 | 0 | 100 | 0 | 0 | 0 | 0 | 0 | 0 | 0 | 0 | 0 | 100 |
| | | *Operculina ?ammonoides* | 0 | 0 | 0 | 0 | 100 | 0 | 0 | 0 | 0 | 0 | 0 | 0 | 0 | 100 |
| | | *Operculina elegans* (shallow) | 0 | 0 | 0 | 0 | 0 | 100 | 0 | 0 | 0 | 0 | 0 | 0 | 0 | 100 |
| | | *Operculina elegans* (deep) | 0 | 0 | 0 | 0 | 0 | 0 | 100 | 0 | 0 | 0 | 0 | 0 | 0 | 100 |
| | | *Operculina complanata* (shallow) | 0 | 0 | 0 | 0 | 0 | 0 | 0 | 100 | 0 | 0 | 0 | 0 | 0 | 100 |
| | | *Operculina complanata* (deep) | 0 | 0 | 0 | 0 | 0 | 0 | 0 | 0 | 100 | 0 | 0 | 0 | 0 | 100 |
| | | *Planoperculina heterosteginoides* | 0 | 0 | 0 | 0 | 0 | 0 | 0 | 0 | 0 | 100 | 0 | 0 | 0 | 100 |
| | | *Planostegina longisepta* | 0 | 0 | 0 | 0 | 0 | 0 | 0 | 0 | 0 | 0 | 100 | 0 | 0 | 100 |
| | | *Planostegina operculinoides* | 0 | 0 | 0 | 0 | 0 | 0 | 0 | 0 | 0 | 0 | 0 | 100 | 0 | 100 |
| | | *Heterostegina depressa* | 0 | 0 | 0 | 0 | 0 | 0 | 0 | 0 | 0 | 0 | 0 | 0 | 100 | 100 |

**Table 5.** Discriminant analysis based on all variables. Correlation matrix between discriminant functions and variables.

| | | discriminant function | | | | | | | | | | | |
|---|---|---|---|---|---|---|---|---|---|---|---|---|---|
| | | 1 | 2 | 3 | 4 | 5 | 6 | 7 | 8 | 9 | 10 | 11 | 12 |
| embracing | *a* | **0.575** | **-0.252** | -0.004 | 0.053 | **0.350** | **0.502** | -0.075 | -0.145 | 0.020 | 0.193 | 0.159 | -0.173 |
| chambers perimeter ratio | $b_0$ | **-0.261** | **-0.672** | **-0.271** | 0.207 | -0.051 | 0.199 | 0.121 | 0.000 | 0.095 | **0.389** | 0.104 | -0.041 |
| chambers perimeter ratio | $b_1$ | **-0.294** | **-0.546** | -0.056 | 0.026 | 0.041 | **0.256** | **0.329** | **0.265** | 0.066 | **0.369** | **0.379** | -0.055 |
| basal chamber length | $b_1$ | -0.099 | -0.138 | **0.429** | **0.279** | -0.233 | -0.096 | -0.038 | **-0.398** | -0.099 | -0.090 | 0.144 | 0.049 |
| chambers backward bend | $b_0$ | 0.064 | **0.268** | **-0.376** | 0.016 | 0.066 | 0.161 | 0.178 | **0.358** | 0.101 | -0.062 | -0.008 | **0.273** |
| mediolateral thickness | $b_1$ | 0.156 | -0.009 | -0.117 | 0.053 | **0.607** | **-0.290** | -0.229 | 0.085 | -0.123 | **0.304** | 0.122 | -0.125 |
| embracing | *p* | 0.049 | 0.190 | **-0.296** | 0.067 | **0.523** | 0.233 | -0.174 | **-0.392** | 0.204 | **0.437** | 0.103 | -0.074 |
| mediolateral thickness | $b_0$ | -0.077 | 0.025 | 0.088 | -0.062 | **-0.504** | 0.167 | **0.248** | -0.194 | **0.324** | -0.106 | -0.163 | **0.448** |
| basal chamber length | $b_0$ | 0.119 | -0.047 | 0.043 | -0.155 | 0.039 | **-0.245** | 0.125 | 0.045 | 0.190 | 0.055 | -0.008 | -0.119 |
| mediolateral thickness | $b_2$ | -0.009 | 0.015 | 0.034 | 0.186 | -0.288 | -0.073 | -0.172 | **0.404** | 0.194 | **0.575** | 0.126 | -0.117 |
| deuteroloculus ratio | | -0.005 | 0.023 | 0.212 | -0.039 | -0.008 | 0.096 | -0.070 | **0.350** | -0.041 | **0.462** | **-0.411** | **0.302** |
| marginal radius | $b_1$ | -0.047 | 0.117 | -0.084 | 0.013 | **-0.344** | 0.139 | -0.221 | -0.041 | 0.078 | 0.054 | **0.672** | 0.143 |
| marginal radius | $b_2$ | -0.136 | **-0.255** | 0.285 | 0.211 | **0.245** | 0.049 | 0.179 | 0.030 | -0.107 | -0.105 | **-0.642** | -0.132 |
| chambers perimeter ratio | $b_2$ | -0.139 | -0.130 | **0.400** | 0.081 | -0.140 | 0.084 | -0.187 | 0.059 | -0.088 | **-0.297** | **0.434** | **0.390** |
| marginal radius | $b_0$ | 0.095 | -0.015 | -0.090 | -0.073 | 0.022 | -0.143 | 0.154 | -0.124 | **-0.298** | **0.304** | 0.019 | **0.529** |
| proloculus size | | 0.097 | -0.018 | -0.160 | -0.112 | -0.058 | -0.023 | 0.020 | -0.214 | -0.092 | 0.171 | -0.114 | **0.494** |
| chambers backward bend | $b_1$ | 0.056 | 0.057 | -0.108 | 0.135 | -0.001 | -0.009 | -0.099 | **-0.240** | -0.083 | **0.244** | **-0.275** | -0.283 |

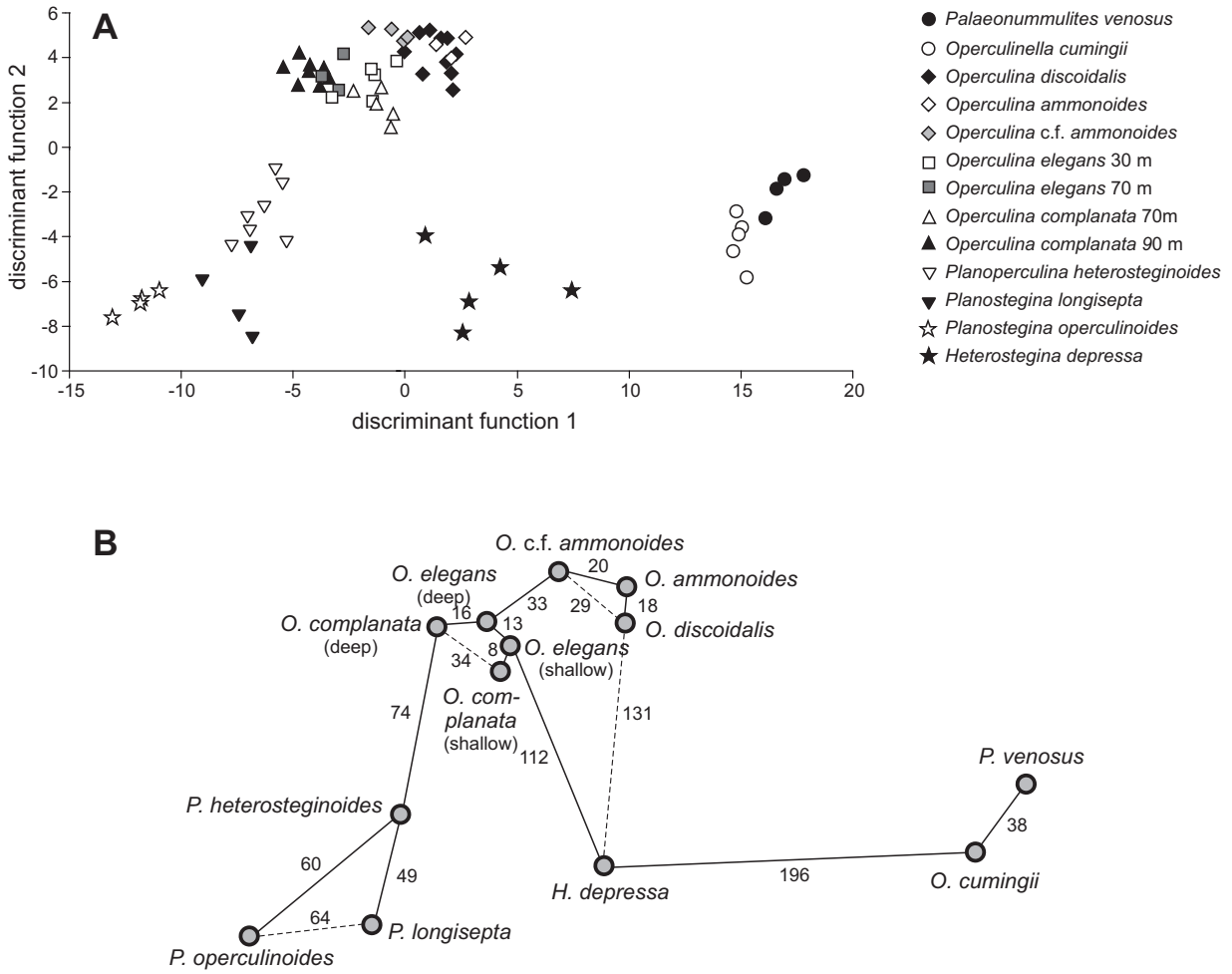


**Figure 10.** Discriminant analysis based on all investigated characters. Position of specimens within the first and second discriminant function (**a**) and shortest Taxonomic Distances (Mahalanobis Distance) between species (**b**).

**Table 6.** Discriminant analysis based on reduced variables including cyclic tests: eigenvalues and variance proportion.

| discriminant function | eigenvalue | % of variance | cumulative % | canonical correlation |
|---|---|---|---|---|
| 1 | 42.361 | 49.2 | 49.2 | 0.988 |
| 2 | 28.776 | 33.4 | 82.6 | 0.983 |
| 3 | 8.871 | 10.3 | 92.9 | 0.948 |
| 4 | 3.482 | 4.0 | 97.0 | 0.881 |
| 5 | 1.024 | 1.2 | 98.2 | 0.711 |
| 6 | 0.740 | 0.9 | 99.0 | 0.652 |
| 7 | 0.483 | 0.6 | 99.6 | 0.571 |
| 8 | 0.240 | 0.3 | 99.9 | 0.440 |
| 9 | 0.063 | 0.1 | 99.9 | 0.243 |
| 10 | 0.052 | 0.1 | 100.0 | 0.223 |
| 11 | 0.012 | 0.0 | 100.0 | 0.111 |

perimeter ratio are not important because the upper and lower limit of this ratio do not differ between these species (Table 9).

*Operculina discoidalis* and *O. ammonoides* differ in the stronger increase of the test spiral in the former species, which exhibits a logistic spiral. This is in contrast to the weak spiral increase in *O. ammonoides*, approximating a spiral of Archimedes. The most significant difference are the pronounced test flattening of *O. discoidalis*, leading to a discus-shaped test, while *O. ammonoides* is the only species showing increasing test thickness in later whorls (Figure 8; Table 9). The differences between *O. ammonoides* and the northern representative *O.* cf. *ammonoides* are – beside strong ribbing in the latter form – are its stronger increase in basal chamber

**Table 7.** Discriminant analysis based on reduced variables including cyclic tests. Comparison of the original (a priori) classification with the predicted classification.

| | | species | predicted classification | | | | | | | | | | | | | | total |
|---|---|---|---|---|---|---|---|---|---|---|---|---|---|---|---|---|---|
| | | | *Palaeonummulites venosus* | *Operculinella cumingii* | *Operculina discoidalis* | *Operculina ammonoides* | *Operculina ?ammonoides* | *Operculina elegans* (shallow) | *Operculina elegans* (deep) | *Operculina complanata* (shallow) | *Operculina complanata* (deep) | *Planoperculina heterosteginoides* | *Planostegina longisepta* | *Planostegina operculinoides* | *Heterostegina depressa* | *Cycloclypeus carpenteri* | |
| original classification | number | *Palaeonummulites venosus* | 4 | 0 | 0 | 0 | 0 | 0 | 0 | 0 | 0 | 0 | 0 | 0 | 0 | 0 | 4 |
| | | *Operculinella cumingii* | 0 | 5 | 0 | 0 | 0 | 0 | 0 | 0 | 0 | 0 | 0 | 0 | 0 | 0 | 5 |
| | | *Operculina discoidalis* | 0 | 0 | 9 | 0 | 0 | 1 | 0 | 0 | 0 | 0 | 0 | 0 | 0 | 0 | 10 |
| | | *Operculina ammonoides* | 0 | 0 | 0 | 3 | 0 | 0 | 0 | 0 | 0 | 0 | 0 | 0 | 0 | 0 | 3 |
| | | *Operculina ?ammonoides* | 0 | 0 | 0 | 0 | 3 | 1 | 0 | 0 | 0 | 0 | 0 | 0 | 0 | 0 | 4 |
| | | *Operculina elegans* (shallow) | 0 | 0 | 0 | 0 | 0 | 4 | 0 | 0 | 1 | 0 | 0 | 0 | 0 | 0 | 5 |
| | | *Operculina elegans* (deep) | 0 | 0 | 0 | 0 | 1 | 0 | 2 | 0 | 0 | 0 | 0 | 0 | 0 | 0 | 3 |
| | | *Operculina complanata* (shallow) | 0 | 0 | 0 | 0 | 1 | 1 | 0 | 3 | 0 | 0 | 0 | 0 | 0 | 0 | 5 |
| | | *Operculina complanata* (deep) | 0 | 0 | 0 | 0 | 0 | 0 | 0 | 0 | 8 | 0 | 0 | 0 | 0 | 0 | 8 |
| | | *Planoperculina heterosteginoides* | 0 | 0 | 0 | 0 | 0 | 0 | 0 | 0 | 0 | 7 | 0 | 0 | 0 | 0 | 7 |
| | | *Planostegina longisepta* | 0 | 0 | 0 | 0 | 0 | 0 | 0 | 0 | 0 | 0 | 4 | 0 | 0 | 0 | 4 |
| | | *Planostegina operculinoides* | 0 | 0 | 0 | 0 | 0 | 0 | 0 | 0 | 0 | 0 | 0 | 4 | 0 | 0 | 4 |
| | | *Heterostegina depressa* | 0 | 0 | 0 | 0 | 0 | 0 | 0 | 0 | 0 | 0 | 0 | 0 | 5 | 0 | 5 |
| | | *Cycloclypeus carpenteri* | 0 | 0 | 0 | 0 | 0 | 0 | 0 | 0 | 0 | 0 | 0 | 0 | 0 | 4 | 4 |
| | percentages | *Palaeonummulites venosus* | 100 | 0 | 0 | 0 | 0 | 0 | 0 | 0 | 0 | 0 | 0 | 0 | 0 | 0 | 100 |
| | | *Operculinella cumingii* | 0 | 100 | 0 | 0 | 0 | 0 | 0 | 0 | 0 | 0 | 0 | 0 | 0 | 0 | 100 |
| | | *Operculina discoidalis* | 0 | 0 | 90 | 0 | 0 | 10 | 0 | 0 | 0 | 0 | 0 | 0 | 0 | 0 | 100 |
| | | *Operculina ammonoides* | 0 | 0 | 0 | 100 | 0 | 0 | 0 | 0 | 0 | 0 | 0 | 0 | 0 | 0 | 100 |
| | | *Operculina ?ammonoides* | 0 | 0 | 0 | 0 | 75 | 25 | 0 | 0 | 0 | 0 | 0 | 0 | 0 | 0 | 100 |
| | | *Operculina elegans* (shallow) | 0 | 0 | 0 | 0 | 0 | 80 | 0 | 0 | 20 | 0 | 0 | 0 | 0 | 0 | 100 |
| | | *Operculina elegans* (deep) | 0 | 0 | 0 | 0 | 33 | 0 | 67 | 0 | 0 | 0 | 0 | 0 | 0 | 0 | 100 |
| | | *Operculina complanata* (shallow) | 0 | 0 | 0 | 0 | 20 | 20 | 0 | 60 | 0 | 0 | 0 | 0 | 0 | 0 | 100 |
| | | *Operculina complanata* (deep) | 0 | 0 | 0 | 0 | 0 | 0 | 0 | 0 | 100 | 0 | 0 | 0 | 0 | 0 | 100 |
| | | *Planoperculina heterosteginoides* | 0 | 0 | 0 | 0 | 0 | 0 | 0 | 0 | 0 | 100 | 0 | 0 | 0 | 0 | 100 |
| | | *Planostegina longisepta* | 0 | 0 | 0 | 0 | 0 | 0 | 0 | 0 | 0 | 0 | 100 | 0 | 0 | 0 | 100 |
| | | *Planostegina operculinoides* | 0 | 0 | 0 | 0 | 0 | 0 | 0 | 0 | 0 | 0 | 0 | 100 | 0 | 0 | 100 |
| | | *Heterostegina depressa* | 0 | 0 | 0 | 0 | 0 | 0 | 0 | 0 | 0 | 0 | 0 | 0 | 100 | 0 | 100 |
| | | *Cycloclypeus carpenteri* | 0 | 0 | 0 | 0 | 0 | 0 | 0 | 0 | 0 | 0 | 0 | 0 | 0 | 100 | 100 |

**Table 8.** Discriminant analysis based on reduced variables including cyclic tests. Correlation matrix between discriminant functions and variables.

| | | discriminant function | | | | | | | | | | |
|---|---|---|---|---|---|---|---|---|---|---|---|---|
| | | 1 | 2 | 3 | 4 | 5 | 6 | 7 | 8 | 9 | 10 | 11 |
| chambers perimeter ratio | $b_0$ | **-0.622** | **0.350** | **0.488** | **-0.269** | **-0.043** | -0.144 | 0.046 | **0.273** | **0.238** | -0.138 | 0.067 |
| embracing | $a$ | **0.430** | **0.695** | **0.422** | -0.230 | -0.078 | -0.075 | **-0.235** | 0.031 | -0.054 | 0.072 | 0.158 |
| chambers perimeter ratio | $b_1$ | **-0.454** | -0.075 | **0.610** | **-0.254** | **-0.248** | 0.213 | -0.165 | **0.317** | 0.119 | -0.169 | **0.274** |
| basal chamber length | $b_1$ | -0.102 | -0.110 | **0.300** | **0.532** | 0.142 | -0.124 | 0.209 | **-0.459** | **0.278** | **-0.468** | 0.134 |
| mediolateral thickness | $b_1$ | 0.168 | 0.119 | 0.066 | **-0.271** | **0.612** | **0.539** | -0.056 | 0.138 | **0.342** | -0.272 | -0.052 |
| mediolateral thickness | $b_2$ | -0.005 | -0.026 | 0.000 | 0.164 | 0.198 | **-0.450** | **-0.311** | **0.700** | 0.159 | -0.156 | **0.308** |
| basal chamber length | $b_0$ | 0.058 | 0.218 | 0.004 | 0.010 | -0.179 | 0.192 | **0.510** | **0.551** | **-0.554** | 0.085 | -0.052 |
| deuteroloculus ratio | | -0.087 | 0.207 | -0.168 | **0.364** | **-0.301** | **0.364** | -0.047 | **0.437** | **0.478** | 0.144 | **-0.351** |
| mediolateral thickness | $b_0$ | -0.091 | -0.026 | -0.082 | 0.210 | **-0.498** | **-0.482** | **0.273** | -0.007 | -0.029 | **0.539** | **0.306** |
| proloculus size | | -0.105 | **0.440** | **-0.286** | 0.070 | **-0.254** | 0.047 | **0.399** | 0.133 | -0.003 | 0.005 | **0.682** |
| chambers perimeter ratio | $b_2$ | -0.169 | -0.001 | 0.119 | **0.455** | -0.145 | **0.255** | -0.040 | **-0.116** | **-0.362** | **0.245** | **0.677** |

length, the thinner tests, test flattening and, last but not least, the clearly evolute test (Table 9).

The visual differentiation between *Operculina elegans* and *O. complanata* is based on septal undulation in large specimens of the latter species. Both species show depth-related test changes. They decrease continuously in both test thickness and initial spiral radius characterizing the embryonic apparatus; at the same time, the expansion rate of the marginal radius increases continuously with depth (Yordanova & Hohenegger 2004). Therefore, both species were separated into shallower (30 and 70 m) and deeper (70 and 90 m) forms. Deeper-living specimens of *O. elegans* are differentiated from shallow-living forms by thinner tests and a higher spiral expansion rate (Yordanova & Hohenegger 2004). *Operculina complanata* shows the same differences between deeper and shallower forms. The additional significant difference in the increase rate of the perimeter ratio (Table 10) is not important because the upper and the lower limit of this character do not differ. Significant differences in both parameters determining the grade of chamber embracing are also unimportant: they are correlated with the higher spiral expansion rate of the margin in deeper individuals, yielding smaller umbilical radii.

Difficulties in differentiating between *O. elegans* and *O. complanata* may be overcome by comparing the shallow representatives of both species on the one hand with the deeper forms on the other hand. While the shallow forms of both species are differentiated solely by the upper limit of chamber perimeter proportion (0.94 in *O. elegans* and 1.01 in *O. complanata*), this difference is insignificant for the deeper-living individuals. Nonetheless, the initial ratio in the chamber perimeters and the acceleration rates differ (Table 10).

This comparison clearly demonstrates that groups of a single species from opposite sites of an environmental gradient (light intensity in *O. elegans* and *O. complanata*) can significantly differ in many parameters. When intermediate forms along the gradient are missing, such ecophenotypes may wrongly be regarded as different species.

The close relationship between *O. elegans* and *O. complanata* at every depth raises the question whether septal undulation (as the single morphological differentiator) really indicates different species or whether it only shows varying reaction of a single species to the environment. Accordingly, proving species differentiation in living forms is

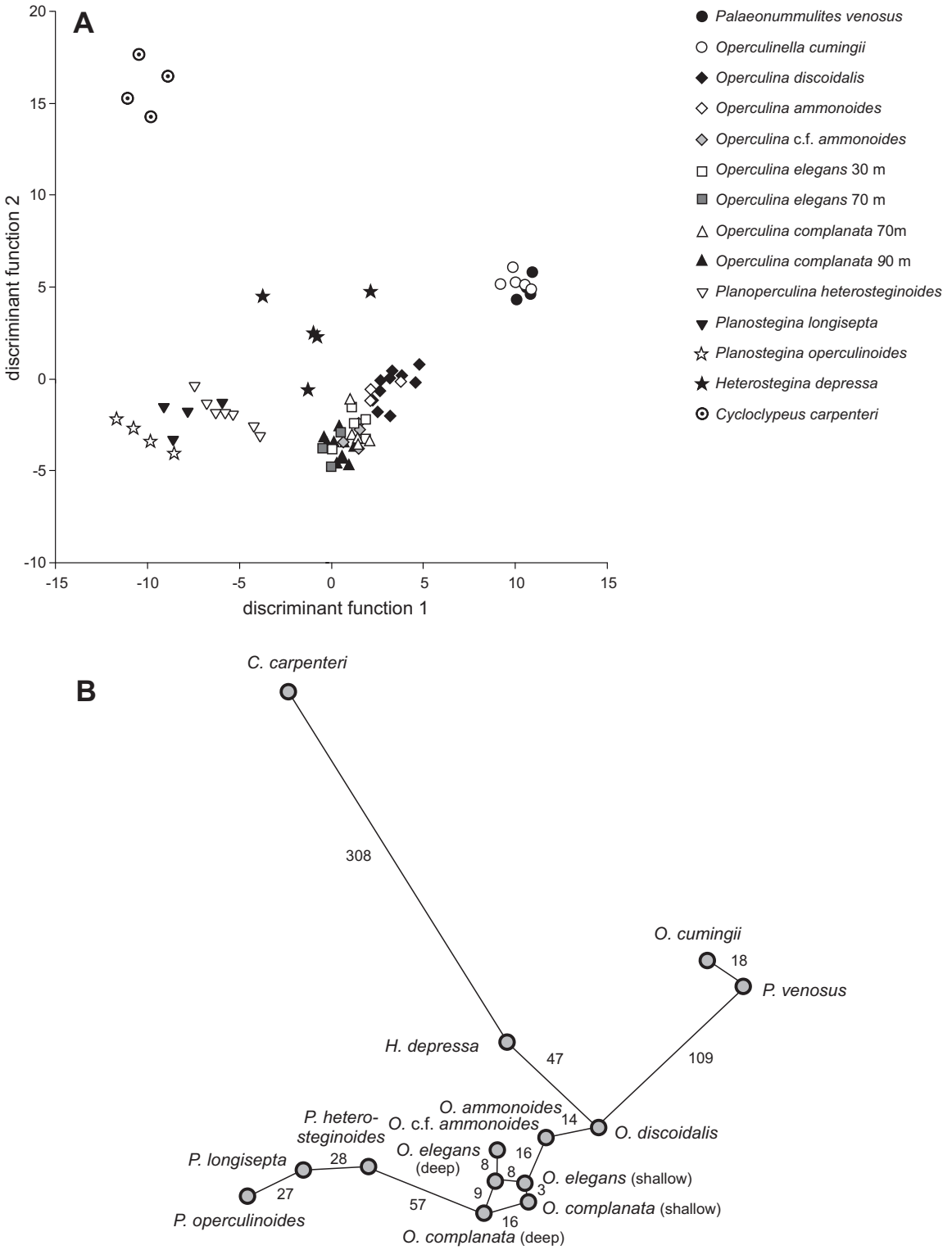


**Figure 11.** Discriminant analysis including *Cycloclypeus carpenteri* reducing the character space. Position of specimens within the first and second discriminant function (**a**) and shortest Taxonomic Distances (Mahalanobis Distance) between species (**b**).

**Table 9.** Differences between pairs of species using analysis of variance.

| comparison | | *Palaeonummulites venosus* / *Operculinella cumingii* | | *Operculina discoidalis* / *Operculina ammonoides* | | *Operculina ammonoides* / *Operculina ?ammonoides* | |
|---|---|---|---|---|---|---|---|
| | | F-value | p(F) | F-value | p(F) | F-value | p(F) |
| proloculus size | | 0.763 | 0.411 | 1.043 | 0.329 | 0.065 | 0.809 |
| deuteroloculus ratio | | 0.015 | 0.905 | 3.116 | 0.105 | 1.320 | 0.303 |
| marginal radius | $b_0$ | 1.793 | 0.222 | 1.980 | 0.187 | 0.017 | 0.903 |
| marginal radius | $b_1$ | 0.001 | 0.978 | 12.442 | 0.005 | 0.575 | 0.482 |
| marginal radius | $b_2$ | 3.808 | 0.092 | 12.608 | 0.005 | 0.304 | 0.605 |
| basal chamber length | $b_0$ | 0.005 | 0.946 | 0.219 | 0.649 | 0.039 | 0.851 |
| basal chamber length | $b_1$ | 5.212 | 0.056 | 2.280 | 0.159 | 7.375 | 0.042 |
| chambers backward bend | $b_0$ | 5.754 | 0.048 | 0.019 | 0.894 | 1.387 | 0.292 |
| chambers backward bend | $b_1$ | 0.113 | 0.747 | 0.037 | 0.850 | 0.268 | 0.627 |
| mediolateral thickness | $b_0$ | 0.141 | 0.719 | 0.693 | 0.423 | 4.729 | 0.082 |
| mediolateral thickness | $b_1$ | 0.144 | 0.715 | 0.622 | 0.447 | 8.011 | 0.037 |
| mediolateral thickness | $b_2$ | 0.474 | 0.513 | 22.328 | 0.001 | 14.067 | 0.013 |
| chambers perimeter ratio | $b_0$ | 3.016 | 0.126 | 1.883 | 0.197 | 1.077 | 0.347 |
| chambers perimeter ratio | $b_1$ | 0.402 | 0.546 | 1.116 | 0.314 | 1.063 | 0.350 |
| chambers perimeter ratio | $b_2$ | 15.959 | 0.005 | 1.909 | 0.194 | 0.904 | 0.385 |
| embracing | $a$ | | | 1.052 | 0.327 | 24.234 | 0.004 |
| embracing | $p$ | | | 1.215 | 0.294 | 2.830 | 0.153 |

only possible by investigating their (sexual or even asexual) reproduction or by molecular genetic analysis (Holzmann *et al.* 2003). If this character is not genetically controlled, then *O. elegans*- and *O. complanata*-morphotypes could be members of a single population or clone.

The two *Planostegina* species differ in the much smaller embryonic apparatus and stronger acceleration rate of the marginal spiral, leading to a rectilinear chamber arrangement in *P. operculinoides*. Further differences are test thickness and the grade of chamber embracement (Table 11). The main differences between *Planoperculina heterosteginoides* and *P. longistepta* are the significantly lower chamber perimeter ratios in the former species, indicating the incomplete chamber partitions by septula (Table 11). The same character separates *Planoperculina heterosteginoides* from *Planostegina operculinoides*. These differences are strengthened by a significantly smaller embryonic apparatus, a higher acceleration rate of the marginal spiral, smaller chamber distances, thinner tests and an earlier onset of the umbilical radius in *P. operculinoides* (Table 11).

## Comparison with Molecular Genetic Investigations

The set of growth-invariant quantitative morphological characters that allow a rather complete reconstruction of the foraminiferal test, especially in nummulitids, can be used to determine the most important characters separating species, ecophenotypes, or both from each other.

Morphological distances between groups point to phylogenetic relationships: They can be compared with

**Table 10.** Differences between pairs of species using analysis of variance.

| comparison | | *Operculina elegans* shallow / *Operculina* elegans deep | | *O. complanata* shallow / *O. complanata* deep | | *Operculina elegans* shallow / *O. complanata* shallow | | *Operculina elegans* deep / *O. complanata* deep | |
|---|---|---|---|---|---|---|---|---|---|
| | | F-value | p(F) | F-value | p(F) | F-value | p(F) | F-value | p(F) |
| proloculus size | | 0.107 | 0.755 | 1.724 | 0.216 | 0.002 | 0.964 | 0.696 | 0.426 |
| deuteroloculus ratio | | 0.791 | 0.408 | 3.322 | 0.096 | 0.098 | 0.762 | 7.863 | 0.021 |
| marginal radius | $b_0$ | 0.495 | 0.508 | 1.684 | 0.221 | 0.227 | 0.646 | 0.493 | 0.500 |
| marginal radius | $b_1$ | 5.056 | 0.066 | 8.520 | 0.014 | 2.600 | 0.146 | 0.766 | 0.404 |
| marginal radius | $b_2$ | 1.288 | 0.300 | 2.262 | 0.161 | 1.764 | 0.221 | 6.263 | 0.034 |
| basal chamber length | $b_0$ | 0.311 | 0.597 | 25.454 | 0.000 | 1.859 | 0.210 | 0.983 | 0.347 |
| basal chamber length | $b_1$ | 0.042 | 0.844 | 22.172 | 0.001 | 0.741 | 0.414 | 3.478 | 0.095 |
| chambers backward bend | $b_0$ | 0.003 | 0.957 | 6.755 | 0.025 | 0.085 | 0.778 | 2.618 | 0.140 |
| chambers backward bend | $b_1$ | 0.036 | 0.856 | 0.293 | 0.599 | 0.067 | 0.803 | 0.429 | 0.529 |
| mediolateral thickness | $b_0$ | 42.910 | 0.001 | 1.650 | 0.225 | 0.900 | 0.370 | 0.123 | 0.734 |
| mediolateral thickness | $b_1$ | 24.247 | 0.003 | 6.913 | 0.023 | 0.360 | 0.565 | 0.120 | 0.737 |
| mediolateral thickness | $b_2$ | 0.008 | 0.932 | 0.269 | 0.614 | 0.011 | 0.918 | 0.120 | 0.737 |
| chambers perimeter ratio | $b_0$ | 1.023 | 0.351 | 2.098 | 0.175 | 4.268 | 0.073 | 0.001 | 0.973 |
| chambers perimeter ratio | $b_1$ | 0.458 | 0.524 | 2.953 | 0.114 | 1.900 | 0.205 | 2.327 | 0.162 |
| chambers perimeter ratio | $b_2$ | 0.176 | 0.690 | 42.056 | 0.000 | 1.332 | 0.282 | 12.342 | 0.007 |
| embracing | $a$ | 2.856 | 0.142 | 14.507 | 0.003 | 0.253 | 0.628 | 2.225 | 0.170 |
| embracing | $p$ | 3.360 | 0.116 | 7.663 | 0.018 | 0.430 | 0.531 | 0.651 | 0.441 |

distances based on molecular genetic investigations (Holzmann *et al.* 2003). The different phylogenetic relationships of *Heterostegina* and *Planostegina*, both partitioning their chambers into chamberlets, as proposed by molecular genetic investigations on small subunits (SSU) of rDNA (Holzmann *et al.* 2003) are now verified by morphogenetic analyses. In both analyses the morphological distances between *Heterostegina* and *Planostegina* are longer than (1) between *Heterostegina* and *Operculinella* in the first analysis (excluding *C. carpenteri*), and (2) between *Heterostegina* and *O. discoidalis* in the second analysis including the cyclic species. This separation of *Heterostegina depressa* from the *Planostegina-Planoperculina* group and the closest connection to *Operculinella cumingii* is manifested by molecular genetic analysis based on SSU rDNA (Holzmann, personal communication 2006). Therefore, placing *Planostegina* and *Heterostegina* into the subfamily Heterostegininae (Banner & Hodgkinson 1991) contradicts the phylogenetic relations based on molecular genetics. However, this placement cannot be verified by complex morphogenetic analyses.

A strange connection based on molecular genetics is that between *Palaeonummulites* and *Planostegina* (Holzmann *et al.* 2003). This relation contradicts the morphometric results based on growth-invariant parameters because the two forms are separated in both analyses by the furthest distance within the discriminant space.

**Table 11.** Differences between pairs of species using analysis of variance.

| comparison | | *Planoperculina heterosteginoides* / *Planostegina longisepta* | | *Planoperculina heterosteginoides* / *Planostegina operculinoides* | | *Planostegina longisepta* / *Planostegina operculinoides* | |
|---|---|---|---|---|---|---|---|
| | | F-value | p(F) | F-value | p(F) | F-value | p(F) |
| proloculus size | | 4.358 | 0.066 | 9.333 | 0.014 | 24.017 | 0.003 |
| deuteroloculus ratio | | 1.091 | 0.323 | 0.063 | 0.808 | 1.907 | 0.217 |
| marginal radius | $b_0$ | 2.841 | 0.126 | 5.536 | 0.043 | 18.354 | 0.005 |
| marginal radius | $b_1$ | 0.029 | 0.868 | 0.488 | 0.503 | 1.821 | 0.226 |
| marginal radius | $b_2$ | 0.856 | 0.379 | 3.257 | 0.105 | 23.448 | 0.003 |
| basal chamber length | $b_0$ | 17.566 | 0.002 | 0.167 | 0.692 | 24.719 | 0.003 |
| basal chamber length | $b_1$ | 17.860 | 0.002 | 0.043 | 0.841 | 15.530 | 0.008 |
| chambers backward bend | $b_0$ | 0.178 | 0.683 | 1.347 | 0.276 | 6.344 | 0.045 |
| chambers backward bend | $b_1$ | 3.037 | 0.115 | 18.589 | 0.002 | 3.476 | 0.112 |
| mediolateral thickness | $b_0$ | 0.859 | 0.378 | 1.536 | 0.247 | 5.244 | 0.062 |
| mediolateral thickness | $b_1$ | 0.334 | 0.578 | 0.221 | 0.650 | 0.945 | 0.368 |
| mediolateral thickness | $b_2$ | 1.613 | 0.236 | 0.713 | 0.420 | 0.284 | 0.613 |
| chambers perimeter ratio | $b_0$ | 8.554 | 0.017 | 13.852 | 0.005 | 0.146 | 0.716 |
| chambers perimeter ratio | $b_1$ | 8.095 | 0.019 | 44.428 | 0.000 | 0.931 | 0.372 |
| chambers perimeter ratio | $b_2$ | 2.460 | 0.151 | 2.478 | 0.150 | 6.737 | 0.041 |
| embracing | $a$ | 0.612 | 0.454 | 8.316 | 0.018 | 4.965 | 0.067 |
| embracing | $p$ | 1.850 | 0.207 | 5.347 | 0.046 | 7.512 | 0.034 |

On the positive side, the unpublished molecular genetic analysis (Holzmann, personal communication 2006) confirms the strong morphological connections between *Operculina discoidalis* and *O. ammonoides*, between *O. elegans* and *O. complanata*, and between *Planoperculina* and *Planostegina*. Morphogenetic connections between *O. discoidalis* and *O. ammonoides* on the one side and between *O. elegans* and *O. complanata* on the other are also confirmed by extremely close molecular relationships. This indicates that the four groups are not species but ecophenotypic groups of the two biological species *O. complanata* and *O. ammonoides*.

With knowledge of ecophenotypic variation, morphometric analyses based on growth-invariant characters yield a more or less complete geometric modelling of the foraminiferal test. This enables the reconstruction of phylogenetic connections even in fossil forms, a reconstruction that may well reflect molecular genetic relationships.

## Acknowledgments

This paper represents results of the Austrian Science Fund Project P 13613-BIO 'Morphocoenoclines and Depth Dependence of Test Characters in Larger

Foraminifera from the West-Pacific'. Thanks are due to the late K. Yamazato, director of the Tropical Biosphere Center, Sesoko Station, University of the Ryukyus, Japan, and to A. Inoue, director of the Research Center for the South Pacific, Kagoshima University, Japan. Also special thanks to my friend, K. Oki, director of the Kagoshima University Museum. All made lengthy stays in Japan and sample collecting during the 1990s possible. I also wish to thank the technical staff of the above institutions and the crew of the Keiten Maru, Kagoshima University, for help in field work. Michael Stachowitsch, a native-English-speaking scientific copyeditor, revised the text.

## References

Banner, F.T. & Hodgkinson, R.L. 1991. A Revision of the foraminferal subfamily *Heterostegininae*. *Revista Espaňola de Micropaleontolgia* **23**, 101–140.

Drooger, C.W. & Roelofsen, J.W. 1982. *Cycloclypeus* from Ghar Hassan, Malta. *Proceedings of the Koninklijke Nederlandse Akademie van Wetenschappen (B)* **85**, 203–218.

Drooger, C.W., Marks, P. & Papp, A. 1971. Smaller radiate *Nummulites* of Northwestern Europe. *Utrecht Micropaleontological Bulletin* **5**, 1–137.

Fermont, W.J.J. 1977a. Biometrical investigation of the genus *Operculina* in Recent Sediments of the Gulf of Elat. *Utrecht Micropaleontological Bulletin* **15**, 111–147.

Fermont, W.J.J. 1977b. Depth-gradients in internal parameters of *Heterostegina* in the Gulf of Elat. *Utrecht Micropaleontological Bulletin* **15**, 149–163.

Hammer, Ø., Harper, D.A.T. & Ryan, P.D. 2001. *PAST: Paleontological Statistics Software Package for Education and Data Analysis*. Palaeontologia Electronica **4**.

Hayward, B.W., Holzmann, M., Grenfell, H.R., Pawlowski, J. & Triggs, C.M. 2004. Morphological distinction of molecular types in *Ammonia* – towards a taxonomic revsion of the world's most commonly misidentified foraminifera. *Marine Mixropaleontology* **50**, 237–271.

Hohenegger, J. 1990. On the way to the optimal suprageneric classification of agglutinating Foraminifera. *In*: Hemleben, C., Kaminski, M., Kuhnt, W. & Scott, D.B. (eds), *Paleoecology, Biostratigraphy, Paleoceanography and Taxonomy of Agglutinated Foraminifera*. Kluwer Academic Publishers, Amsterdam, 77–104.

Hohenegger, J. 1994. Determination of Upper Triassic and Lower Jurassic Ichthyolarias using morphogenetic programs. *Micropaleontology* **39**, 233–262.

Hohenegger, J. 2000. Coenoclines of larger foraminifera. *Micropaleontology* **46**, supplement no. 1, 127–151.

Hohenegger, J. 2004. Depth coenoclines and environmental considerations of Western Pacific larger foraminifera. *Journal of Foraminiferal Research* **34**, 9–33.

Hohenegger, J. & Tatzreiter, F. 1992. Morphometric methods in determination of ammonite species, exemplified through *Balatonites* shells (Middle Triassic). *Journal of Paleontology* **66**, 801–816.

Hohenegger, J., Yordanova, E. & Hatta, A. 2000. Remarks on West Pacific Nummulitidae (Foraminifera). *Journal of Foraminiferal Research* **30**, 3–28.

Holzmann, M., Hohenegger, J. & Pawlowski, J. 2003. Molecular data reveal parallel evolution in nummulitid Foraminifera. *Journal of Foraminiferal Research* **33**, 8–15.

Krzanowski, W.J. & Marriott, F.H.C. 1995. *Multivariate Analysis. Part 2. Classification, Covariance Structures and Repeated Measurements*. Arnold, London.

Less, G., Özcan, E., Papazzoni, C.A. & Stockar, R. 2008. The middle to late Eocene evolution of nummulitid foraminifer *Heterostegina* in the Western Tethys. *Acta Palaeontologica Polonica* **53**, 317–350.

Mayr, E. & Ashlock, P.D. 1991. *Principles of Systematic Zoology*. McGraw-Hill, New York.

Özcan, E., Less, G., Báldi-Beke, M., Kollányi, K. & Acar, F. 2009. Oligo–Miocene foraminiferal record (Miogypsinidae, Lepidocyclinidae and Nummulitidae) from the Western Taurides (SW Turkey): biometry and implications for the regional geology. *Journal of Asian Earth Sciences* **34**, 740–760.

Pecheux, M.J.F. 1995. Ecomorphology of a recent large foraminifer, *Operculina ammonoides*. *Geobios* **28**, 529–566.

Schaub, H. 1981. *Nummulites et Assilines de la Tèthys paléogène. Taxinomie, phylogénese et biostratigraphie*. Mémoires Suisses de Paléontologie **104-106**.

Serra-Kiel, J., Hottinger, L., Caus, E., Drobne, K., Ferrandez, C., Jauhri, A.K., Less, G., Pavlovec, R., Pignatti, J.S., Samso, J.M., Schaub, H., Sirel, E., Strougo, A., Tambareau, Y., Tosquella, J. & Zakrevskaya, E. 1998. Biostratigraphy of the Tethyan Paleocene and Eocene. *Bulletin Societe géologique de France* **129**, 1–19.

Sneath, P.H.A. & Sokal, R.R. 1973. *Numerical Taxonomy*. W.H. Freeman and Company, San Francisco.

SPSS 15.0.1 for Windows 2006.

Yordanova, E.K. & Hohenegger, J. 2004. Morphocoenoclines of living operculinid foraminifera based on quantitative characters. *Micropaleontology* **50**, 149–177.